Recent Progresses in Soft X-ray Emission Spectroscopy

M.Terauchi[1], T.Hatano[1], M.Koike[2], A.S.Pirozhkov[2], H.Sasai[3], T.Nagano[3], M.Takakura[4] and T.Murano[4]

[1]Tohoku University, [2]National Institutes for Quantum and Radiological Science and Technology, [3]SHIMADZU Corp., [4]JEOL Ltd.

Contents

1. Introduction; X-ray emission & soft X-ray
2. SXES of light elements and its characteristics
3. Information in L-emissions of 3d transition metal elements
4. SXES with mapping (EPMA)
5. Improvements in SXES electron microscopy

(SXES: soft X-ray emission spectroscopy)

We have been introduced and improving SXES instrument for electron microscope.

1. Introduction; X-ray emission & soft X-ray

Basics of X-ray emission spectroscopy

X-ray emission

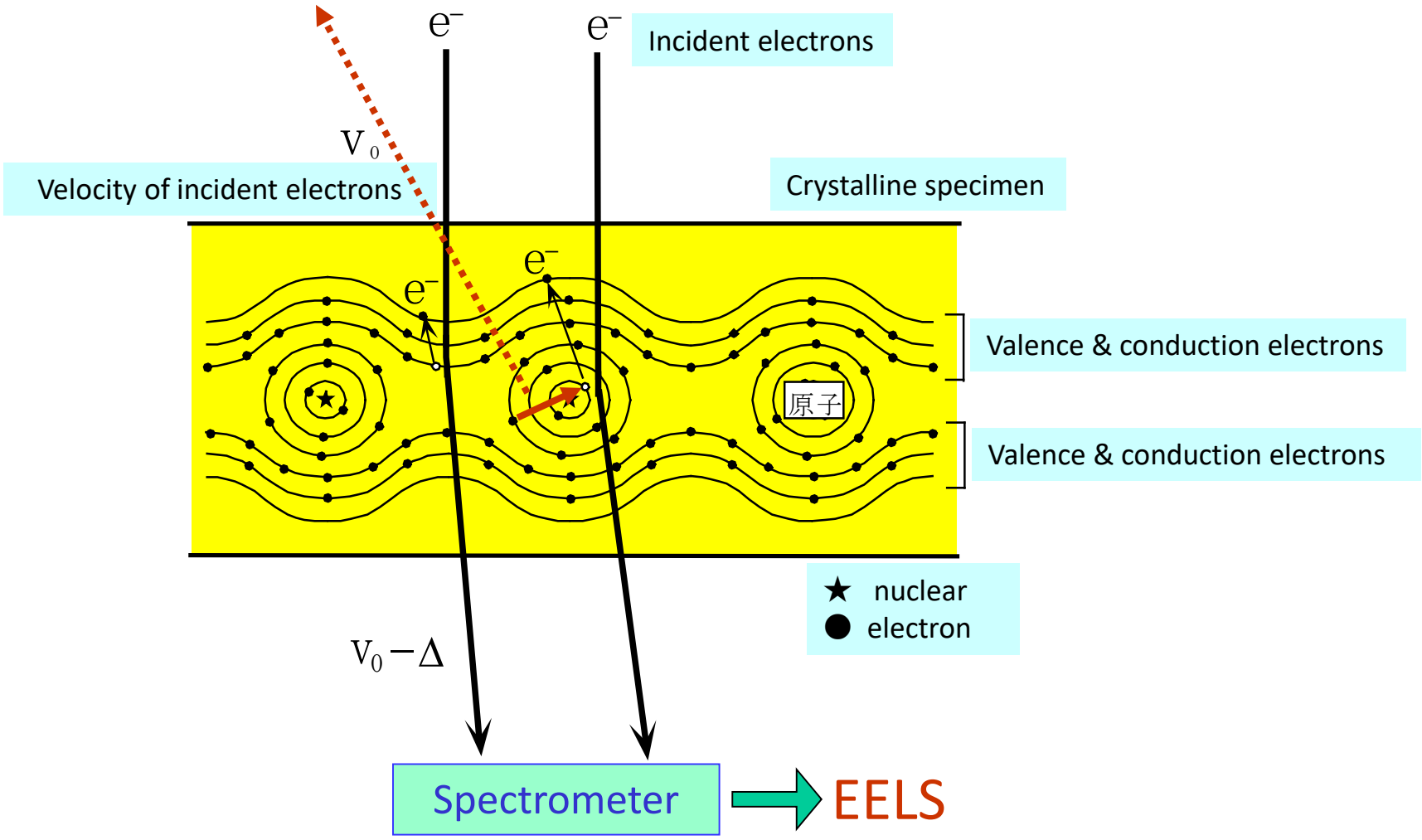

EM-based Spectroscopies

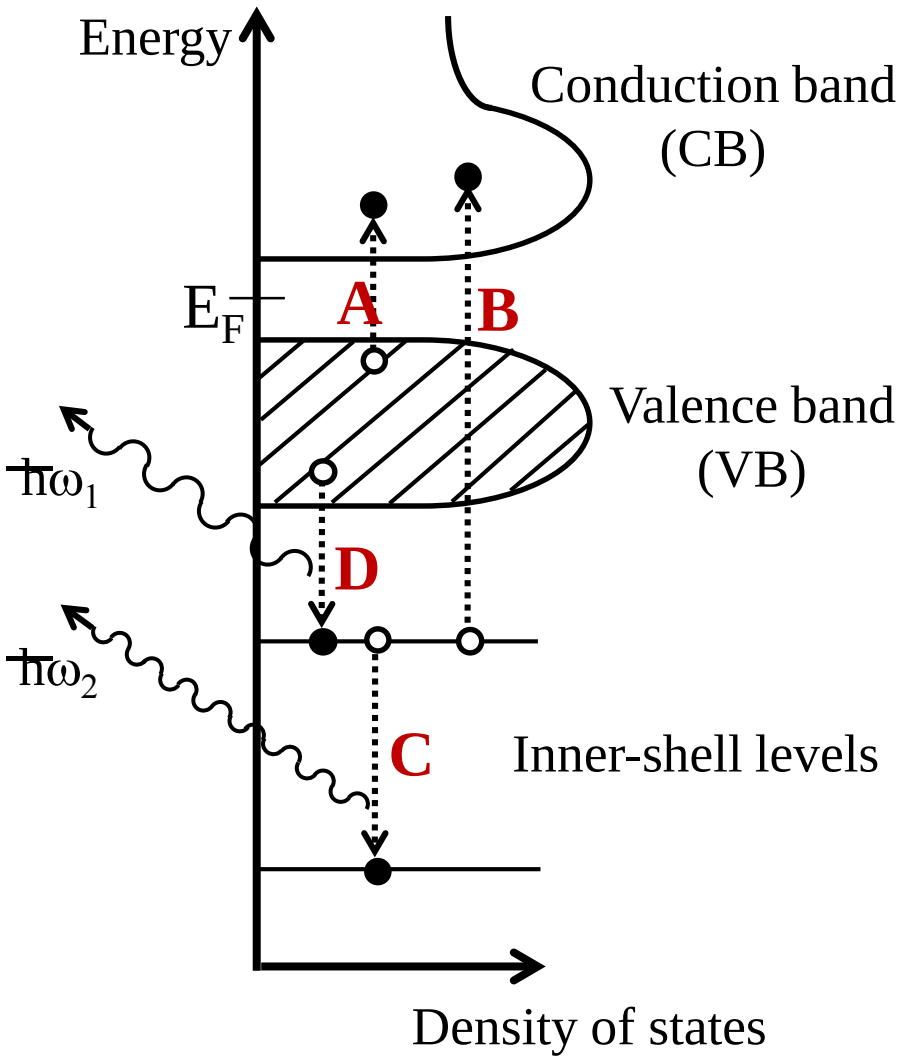

EELS: Electron Energy-loss Spectroscopy
SXES: Soft X-ray Emission Spectroscopy

A: EELS : Valence-loss (ε, J_{DOS})
⇔ Optical measurements

ΔE<0.2eV

B: EELS : Core-loss (DOS of CB)
⇔ XAS, IPES

C&D: XES : Composition
(EDS: ΔE~130eV)

D: SXES : ΔE<1eV ⇒ pDOS of VB
⇔ XES(SOR), PES

Application field of EM-SXES

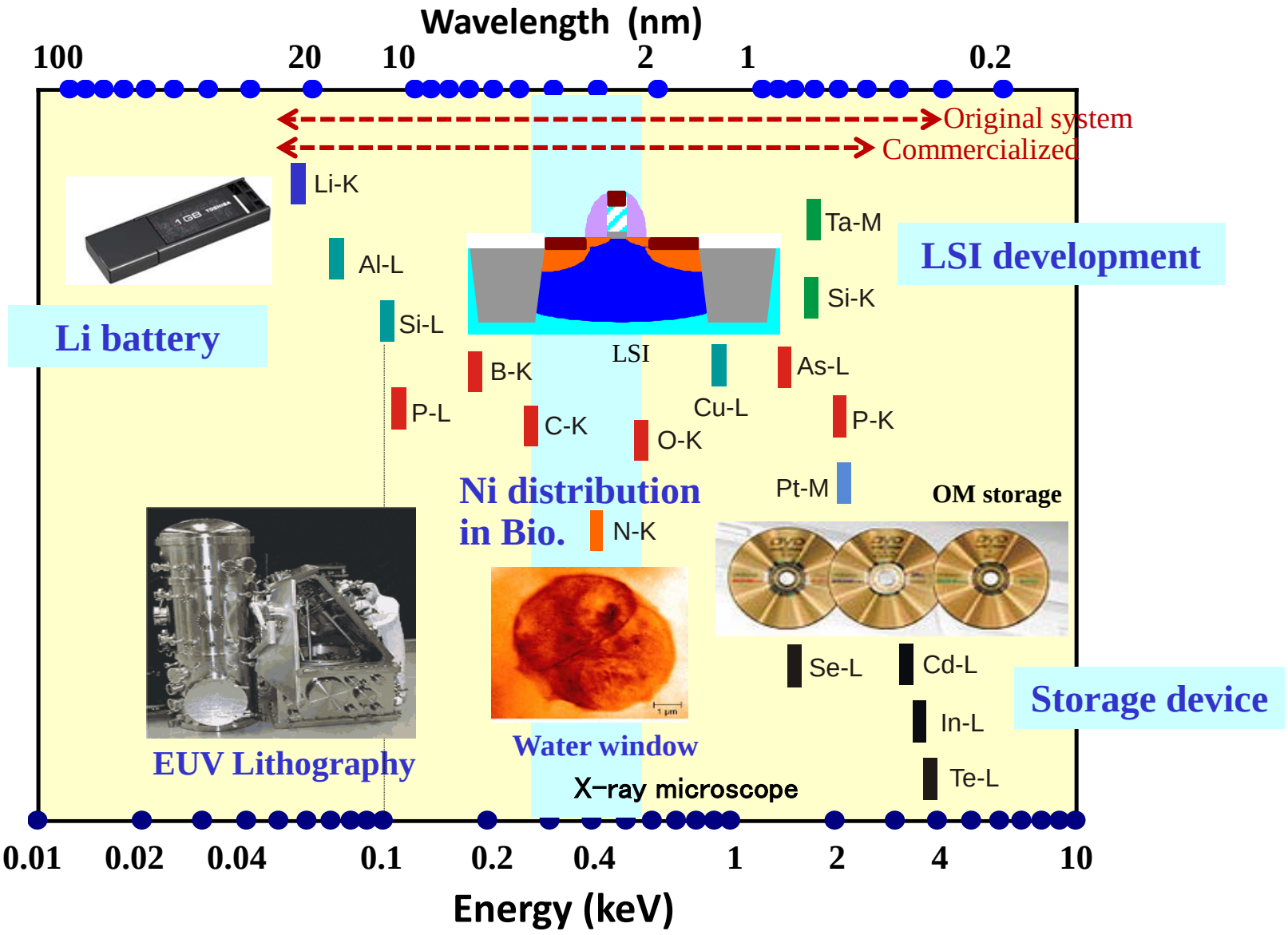

2. SXES of light elements and its characteristics

Conventional XES in TEM: EDS

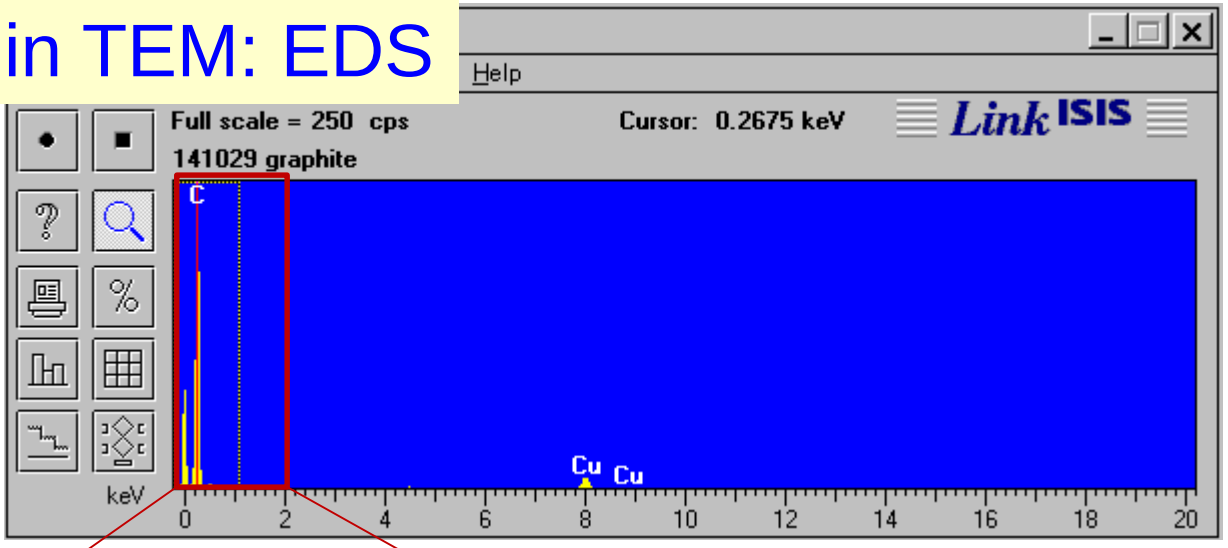

C-K emission : VB(bonding electron; 2p) → C1s

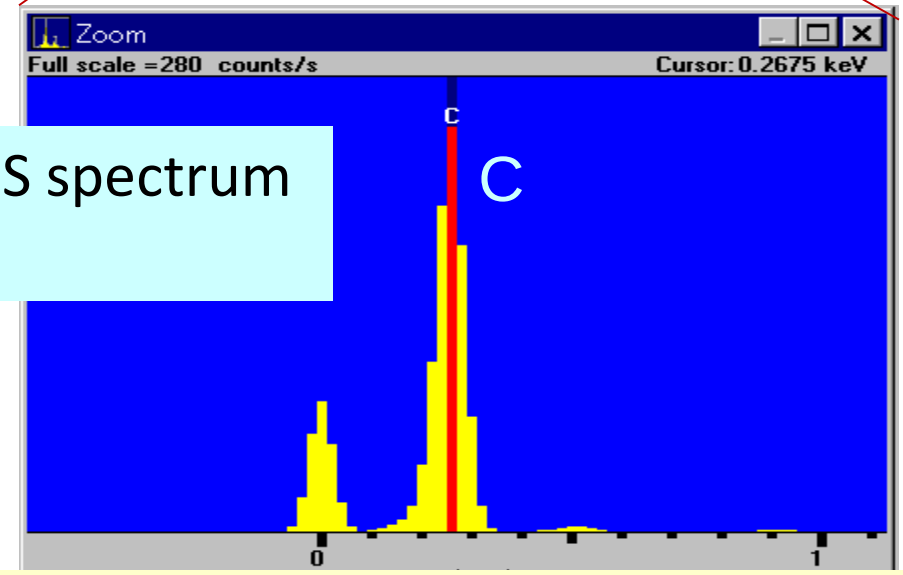

Conventional EDS spectrum of graphite

No chemical-bond information due to a low energy-resolution

High energy-resolution XES with TEM

K-emission: VB(2p)→1s, *p*-symmetry DOS (dipole selection rule)

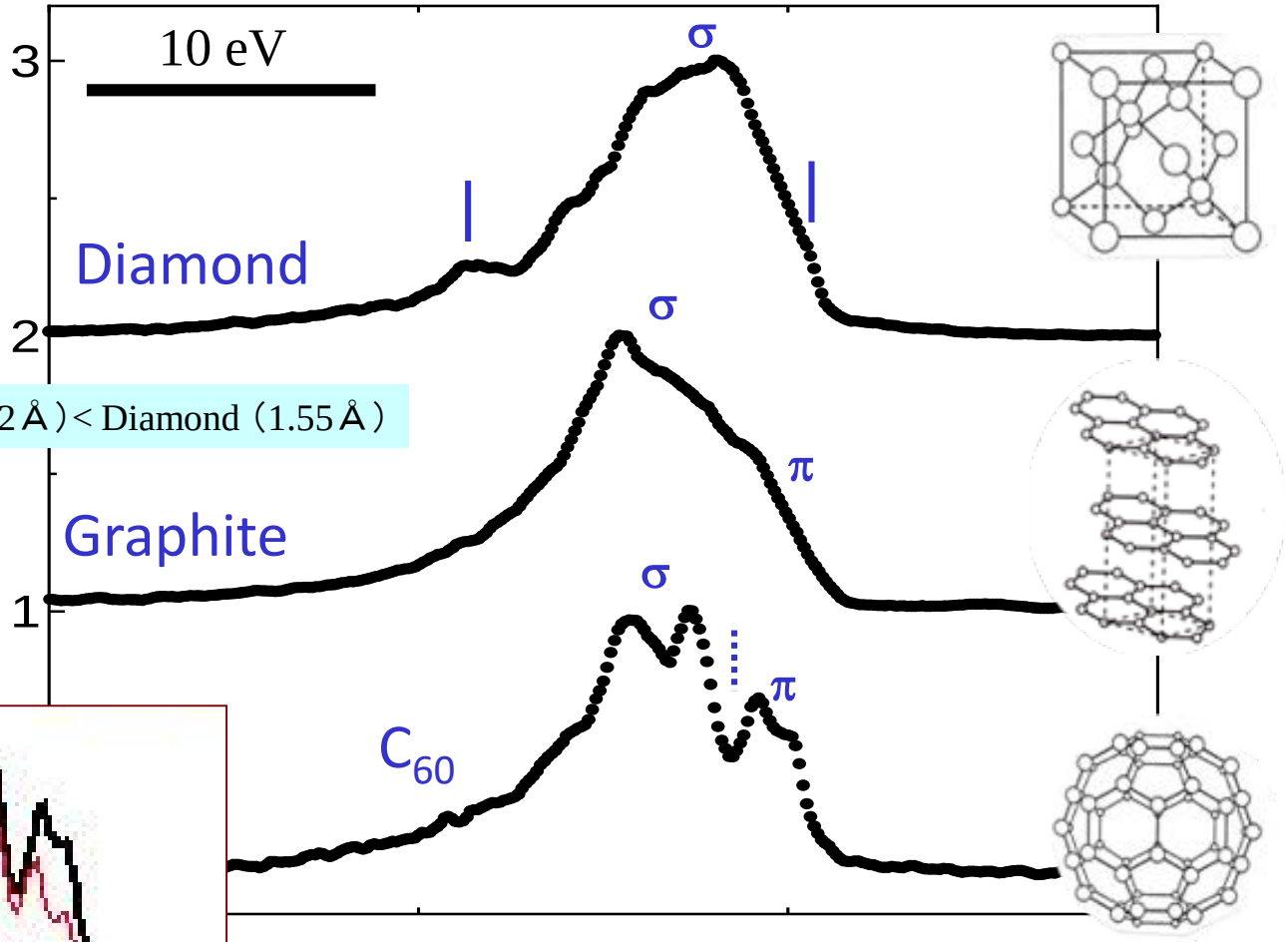

σ-bond length : Graphite（1.42 Å）< Diamond（1.55 Å）

Data obtained at ALS

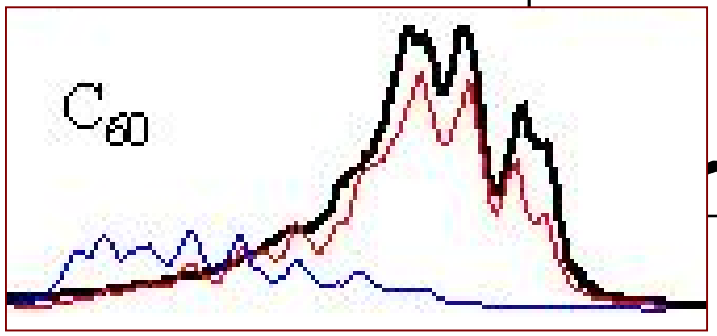

C_{60} crystal : Prof. Yamanaka (Hiroshima Univ.)

M.Terauchi, *et al.*, *J. Electron Microscopy* **59,** 251 (2010).

At the beginning of EM-SXES development

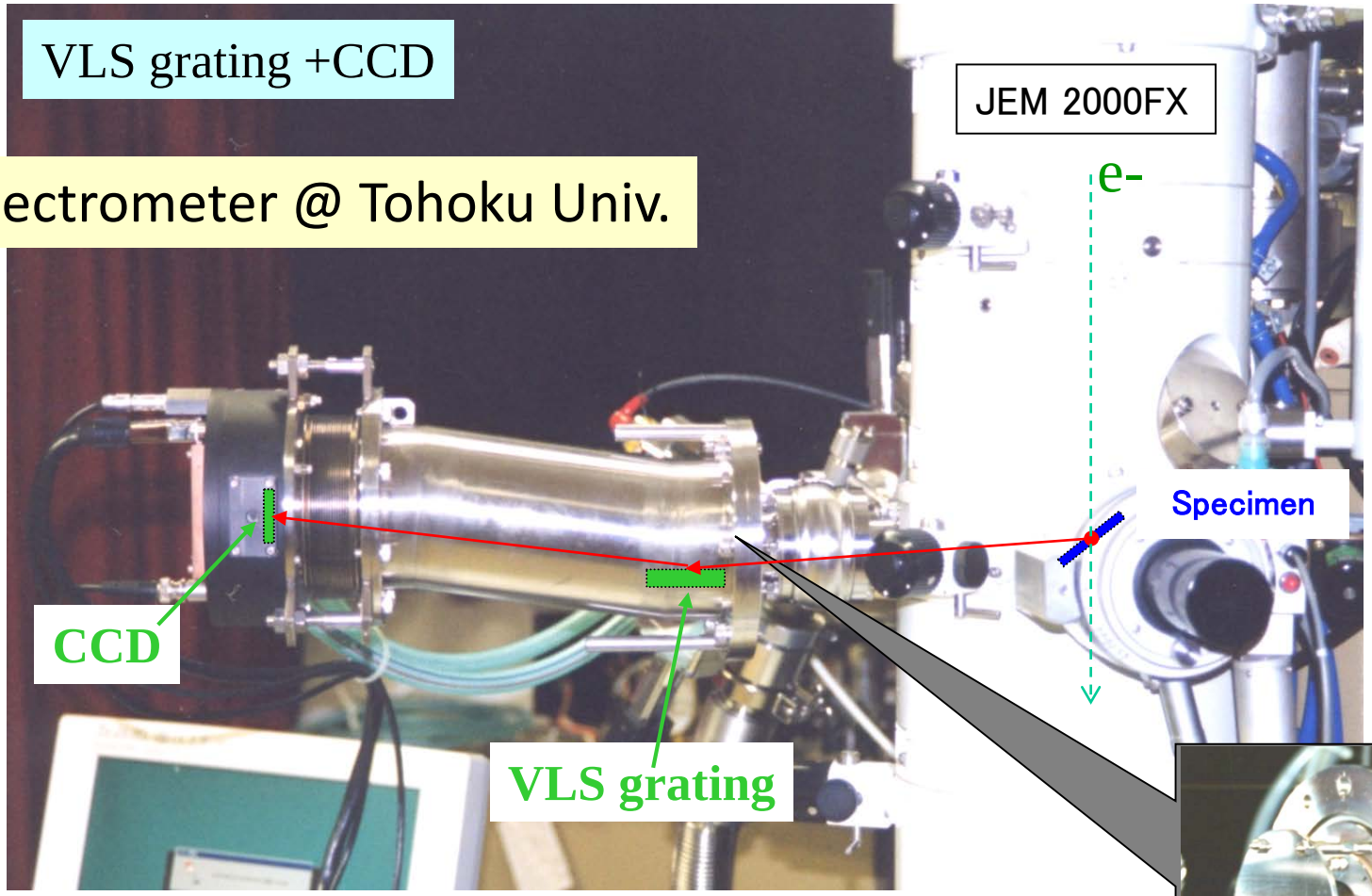

M.Terauchi, *et al.*, *J. Electron Microscopy* **50,** 101 (2001).

Original design of this optics : T.Harada and T.Kita, Applied Optics, 19, 3987 (1980)

EDS of h-BN

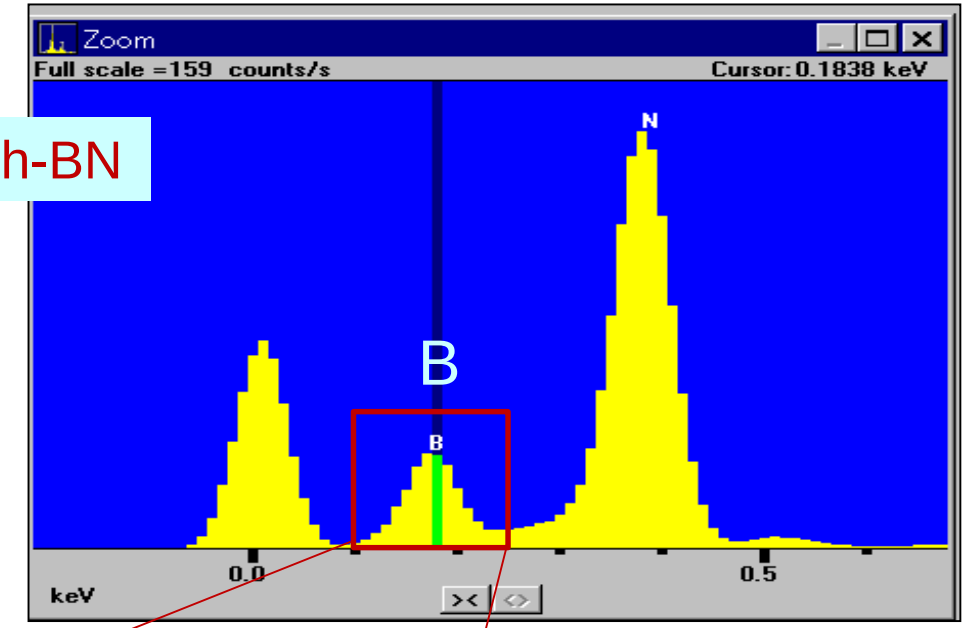

TEM-SXES: bonding information with microscopy

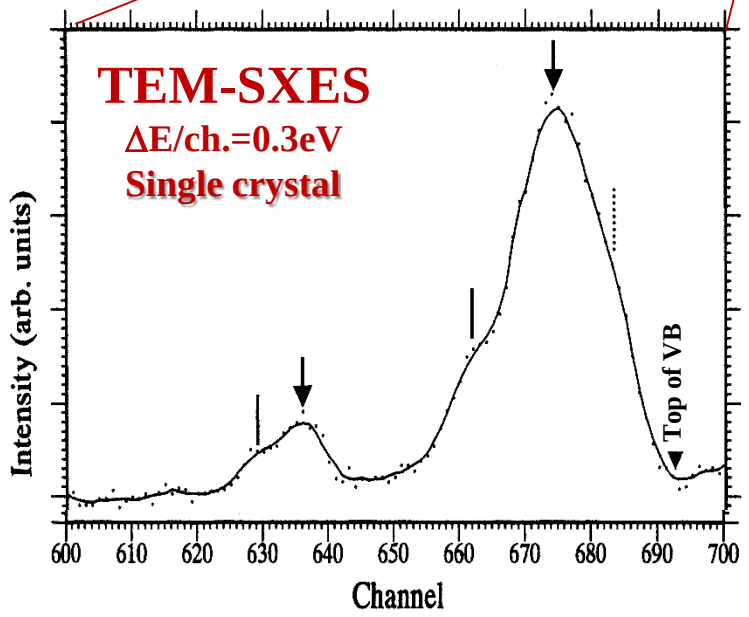

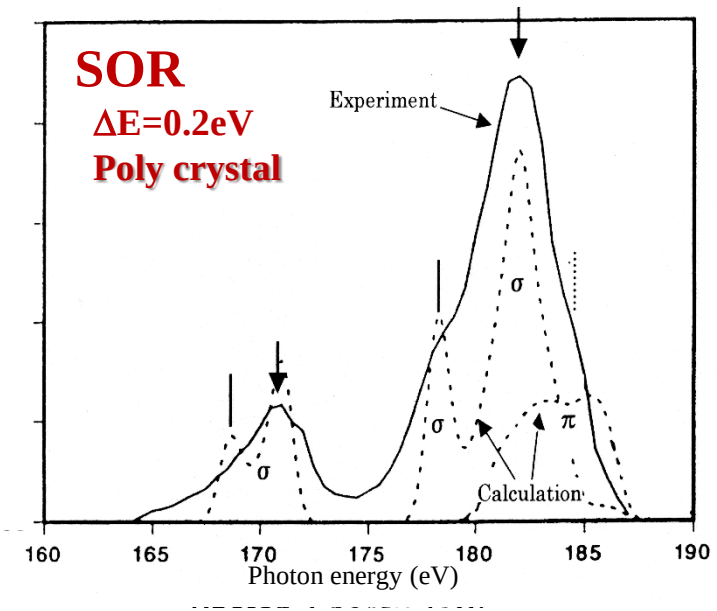

Correspondence between experiment and electronic transition in a material

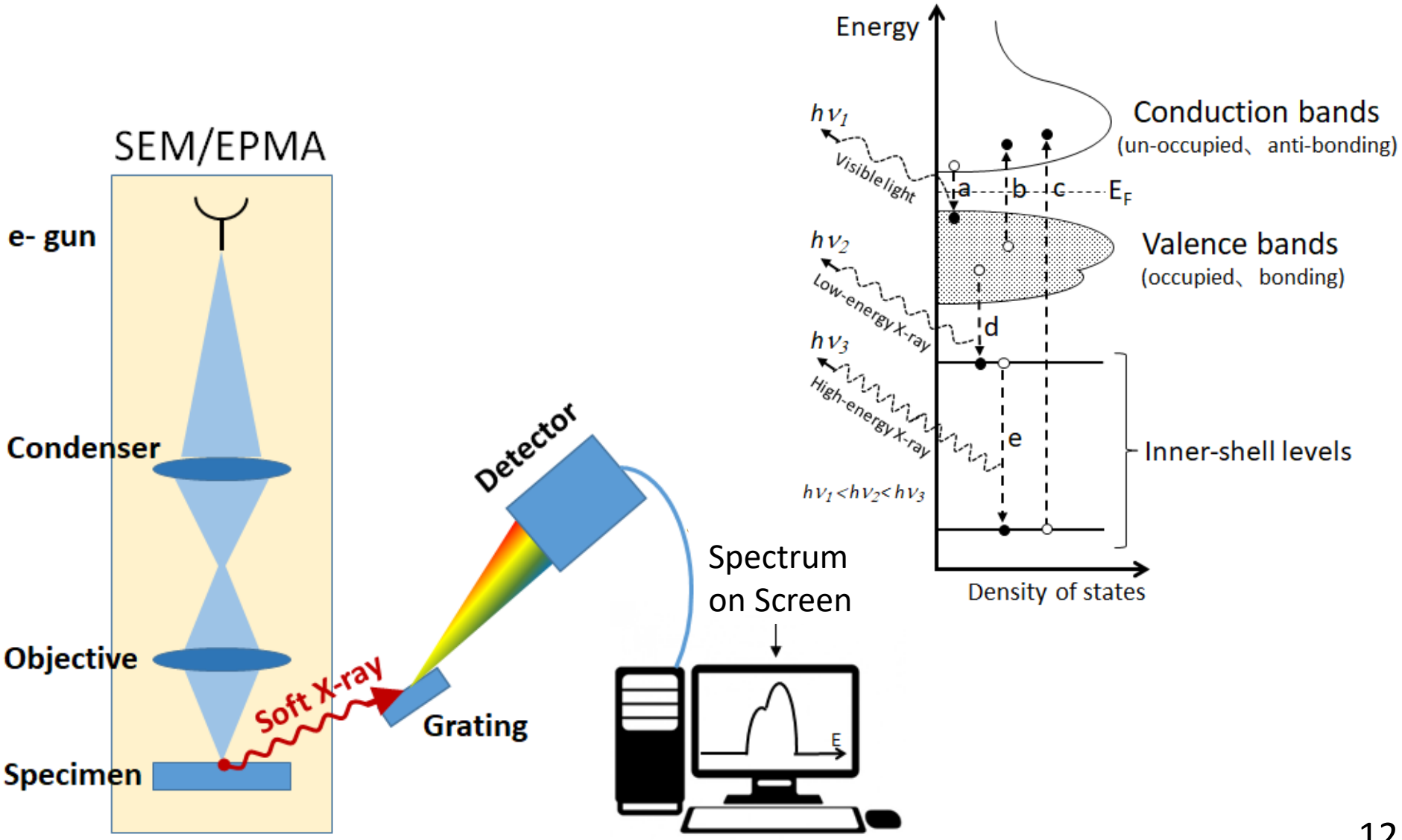

Example: B-K emissions of boron materials

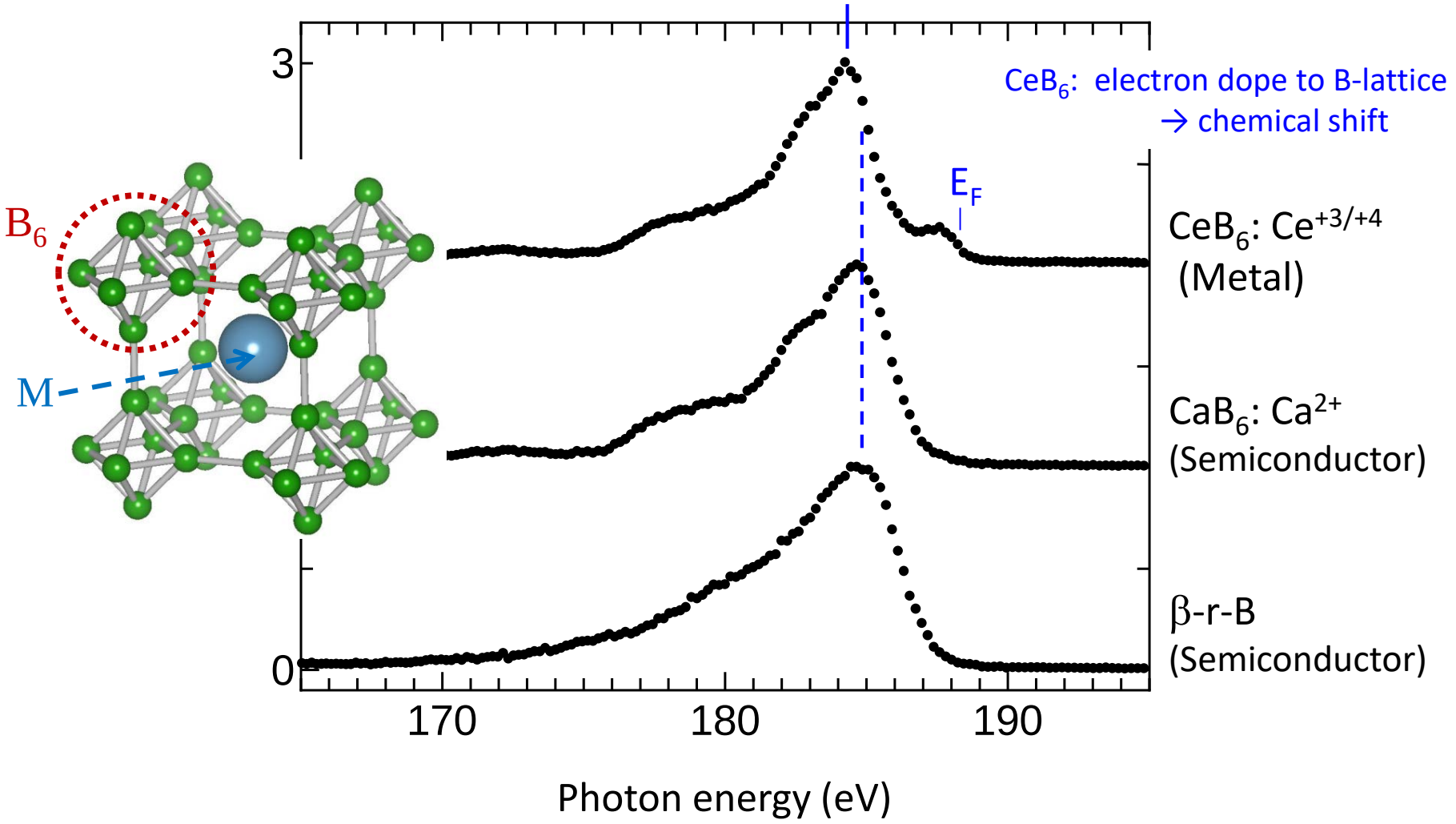

SXES spectrum shows what ?
- Si-L emission -

Band diagram of Si
（calculation）

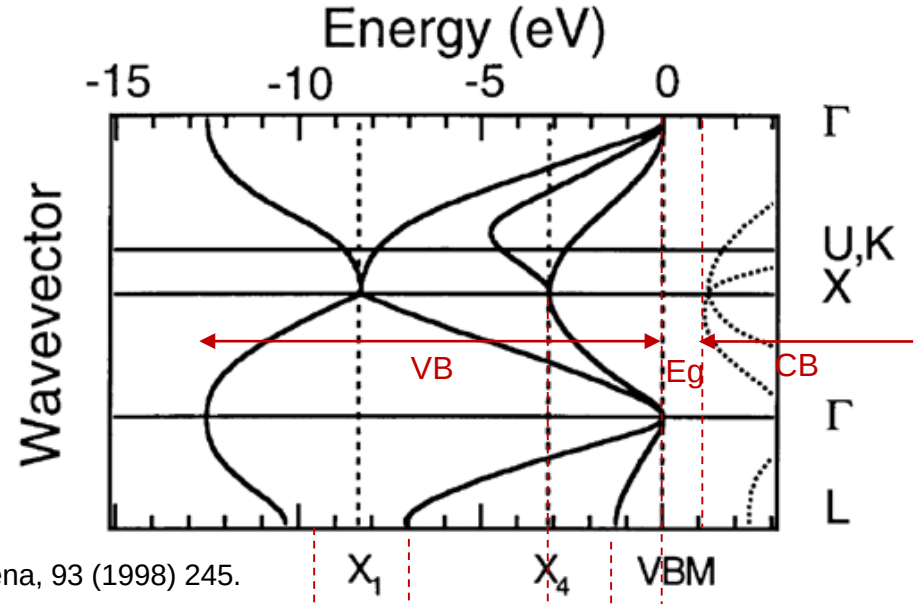

S. Eisebitt, et al.,
J. Electron Spec. and Rel. Phenomena, 93 (1998) 245.

SOR-SXES →

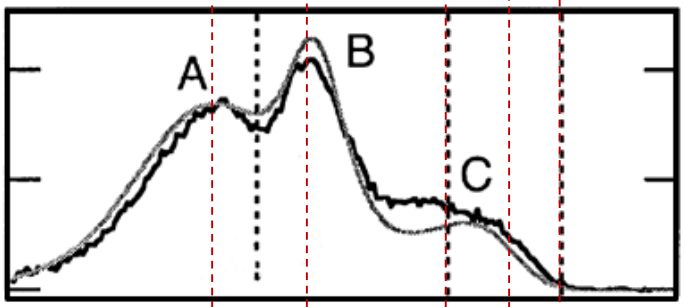

Energy spread of VB < ~10eV
↓
ΔE < 1eV is necessary for bonding state analysis

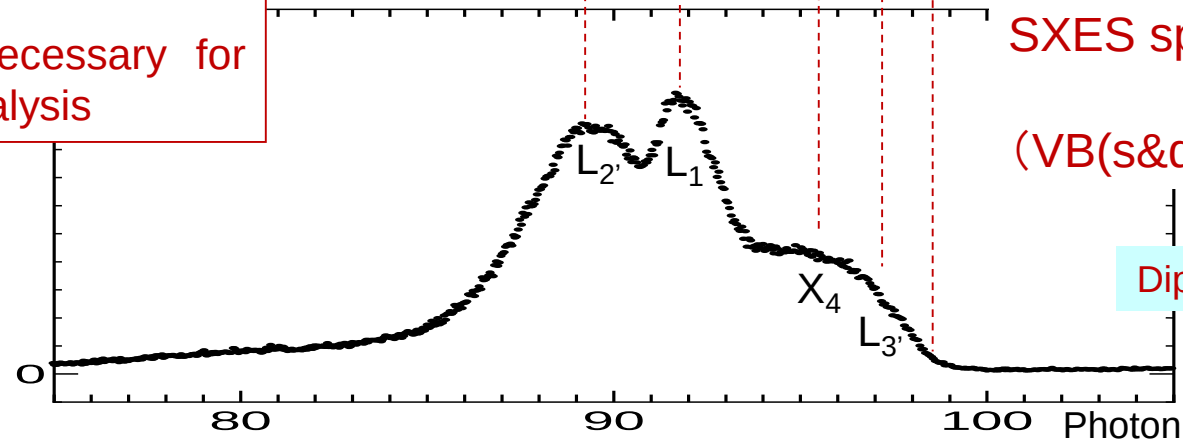

SXES spectrum of SEM-SXES
（VB(s&d) → 2p）

Dipole selection rule

Effect of dipole selection rule on XES spectrum

Experimental spectrum Si-L

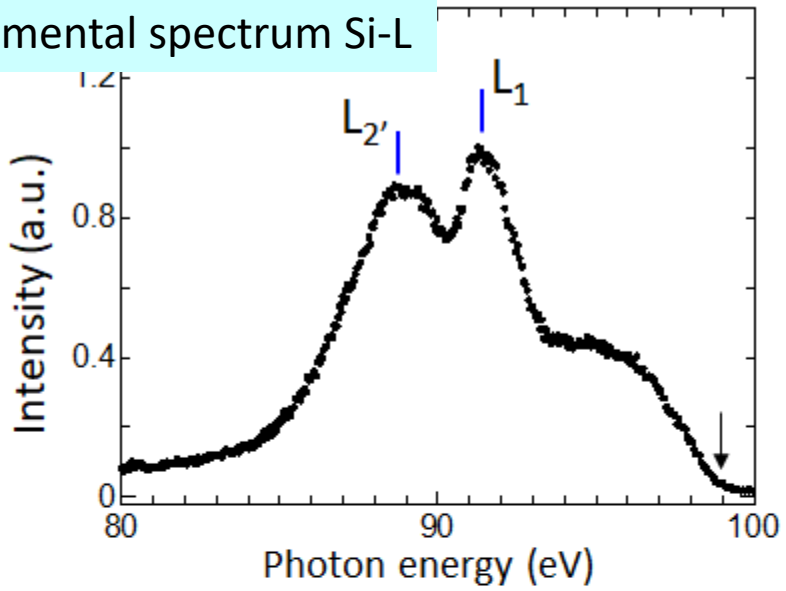

Dipole allowed DOS
can be observed.

Calculated DOS of Si

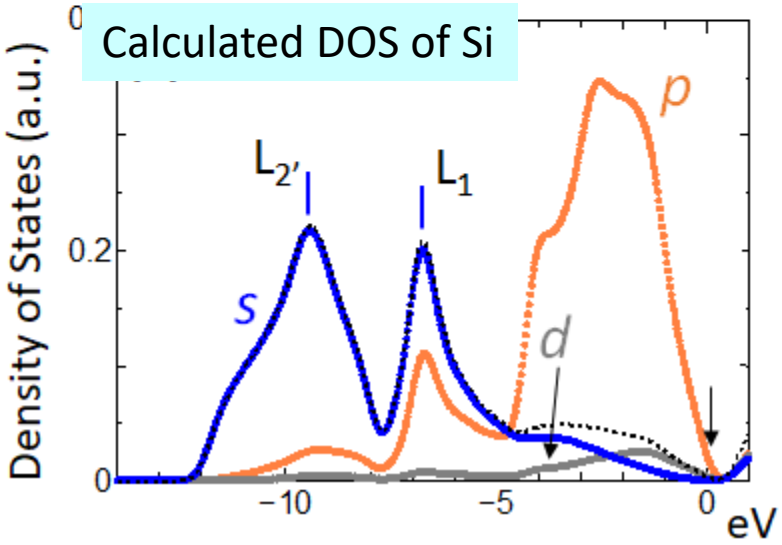

Si-L ($L_{2,3}$: $2p_{1/2}$&$2p_{3/2}$)
↓
s+d symmetry can be observed

3. Information in L-emissions of 3d transition metal elements

SXES spectrometer (ver.7) attached to a SEM

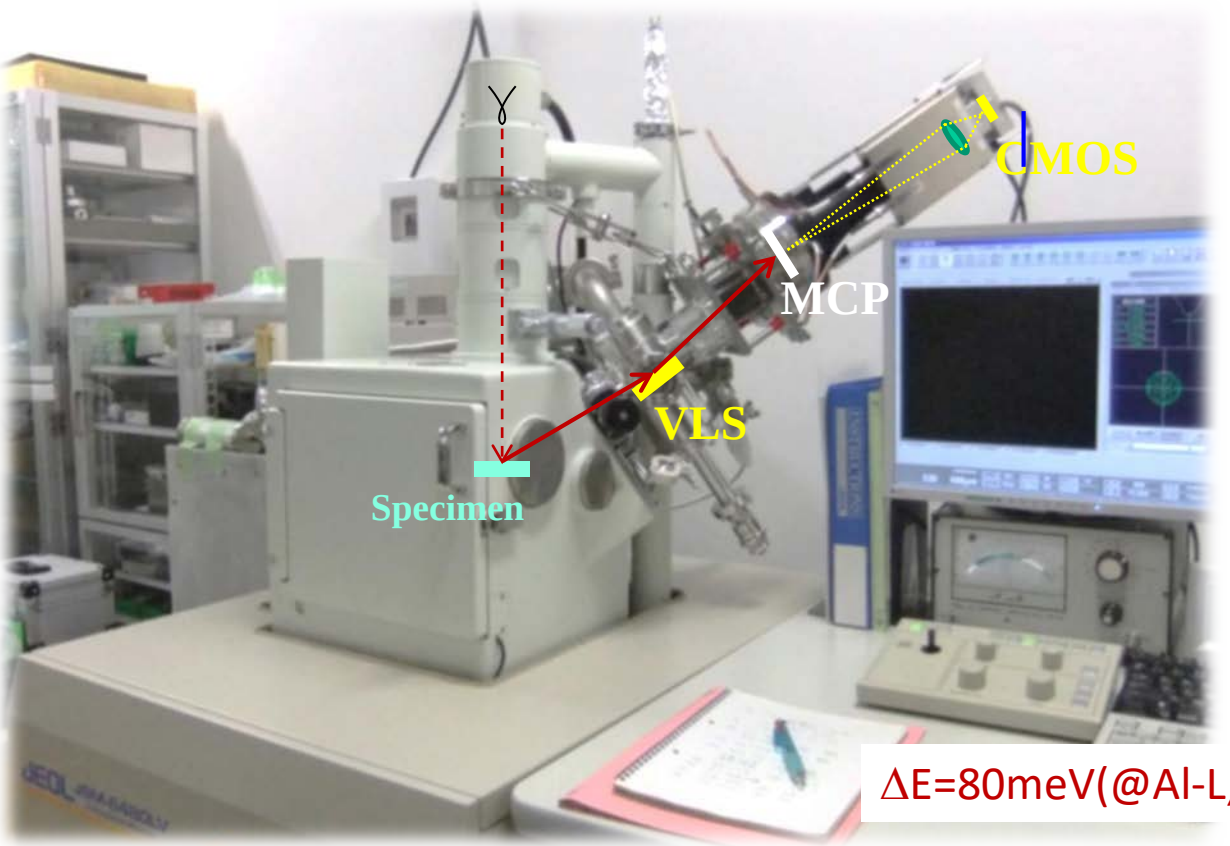

Specimen stage

ΔE=80meV(@Al-L, E/ΔE~900)

SEM: JSM-6480LV

Acc. voltage: 0.3 kV - 30 kV

Cathode: W-filament

Vac. system: DP + RP

SXES instrument: ver.7 @Tohoku

Gratings: JS50XL, JS200N, JS2000, JS4000

Energy range: 50 eV – 4000 eV

Detector: Fine-pixel MCP + CMOS camera

Detection: Photon counting mode

M.Terauchi *et al., Microsc. Microanal*. **20** (2014) 692, **22(Suppl 3)** (2016) 414.

SXES spectra of Ti-O materials

- O-K, Ti-Lαβ, Ti-Lℓη are clearly resolved.
- Shoulder structures of bonding are seen.

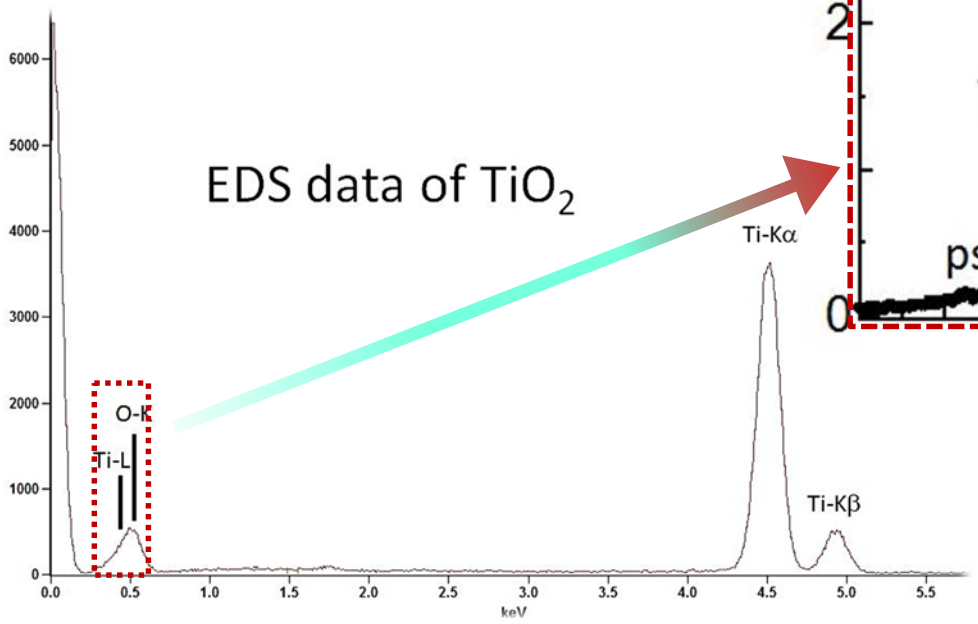

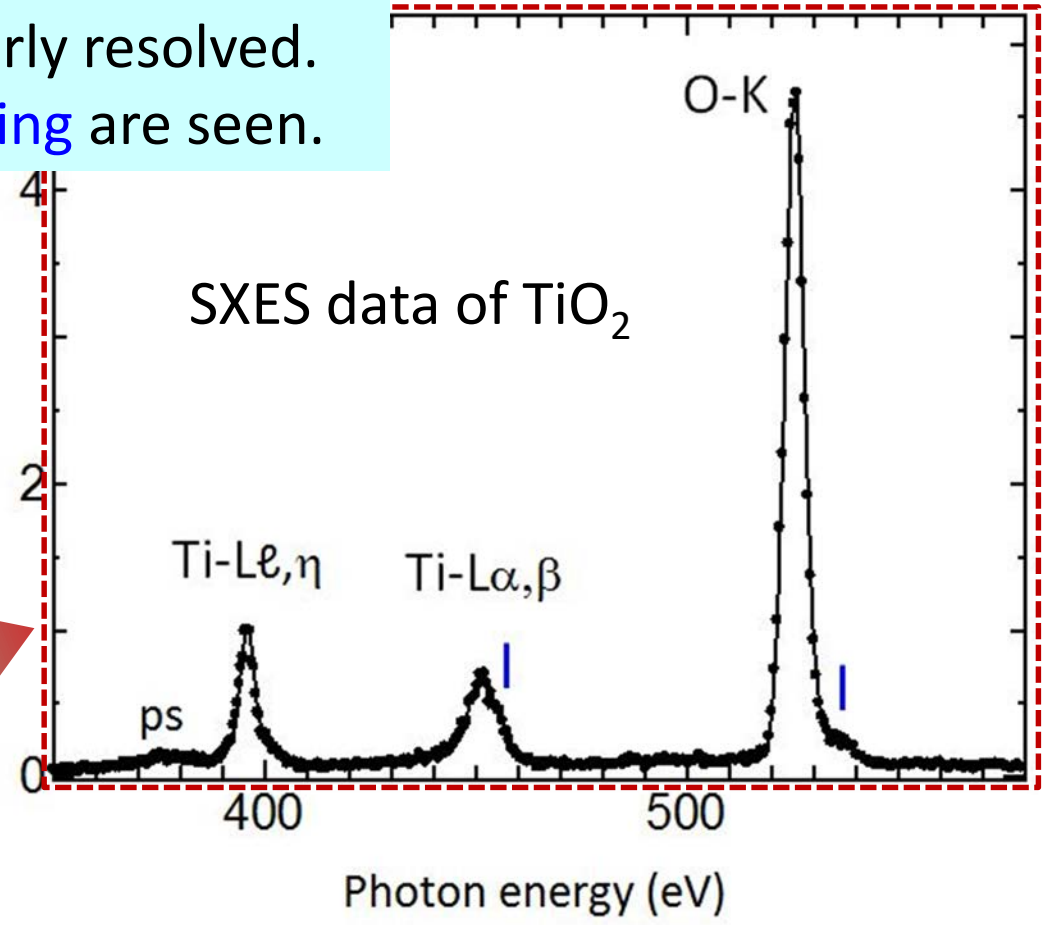

Ti-Lα,β emissions with different valency

Ti-Lα: $3d_{5/2,3/2} \rightarrow 2p_{3/2}$

Ti-Lβ: $3d_{3/2} \rightarrow 2p_{1/2}$

VB-DOS + Chem. shift

TiO2 is pure ionic material → No Ti-L emission
→ covalent component is observed

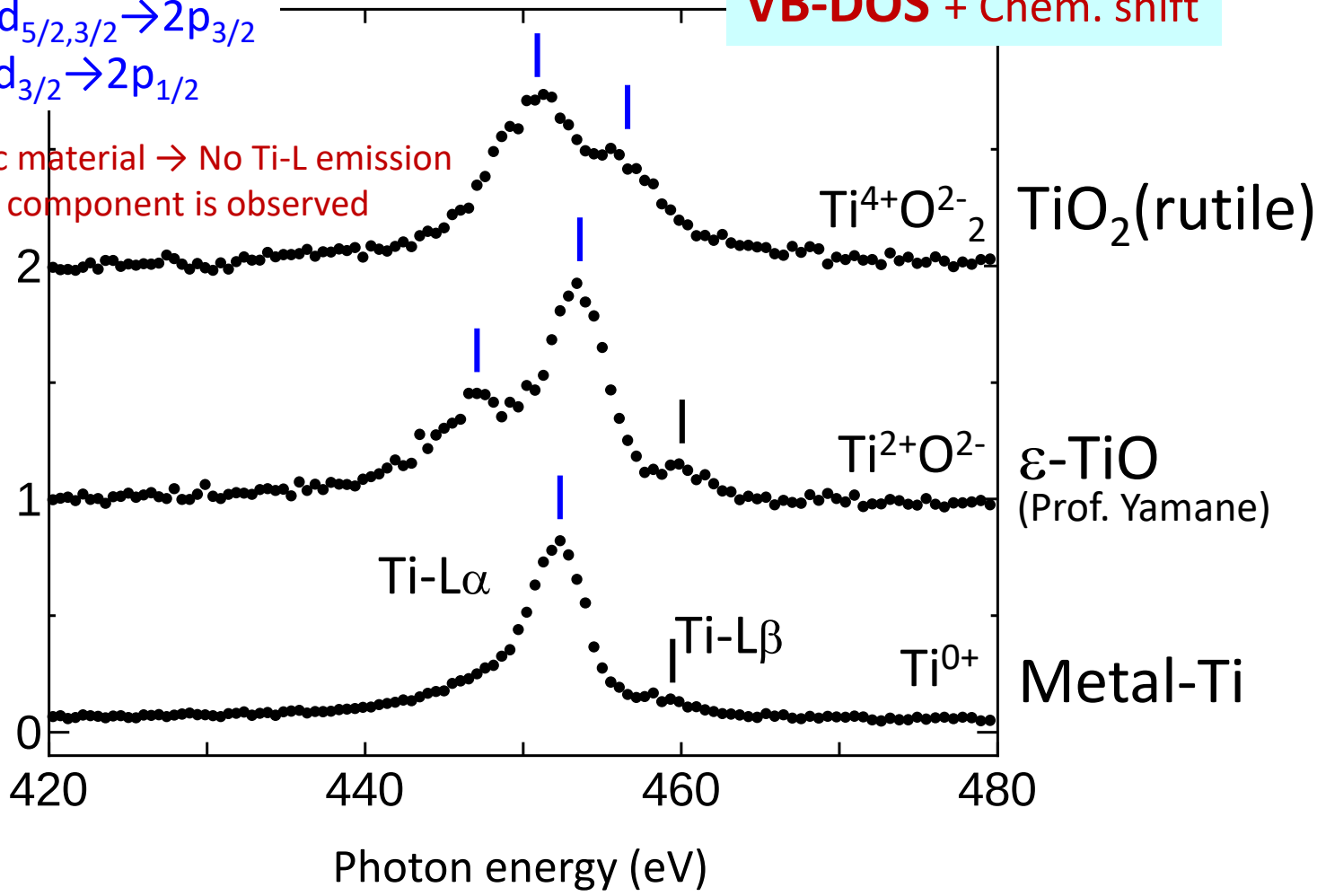

Different intensity distributions → different bonding states

Ti-Lℓ,η emissions with different valency

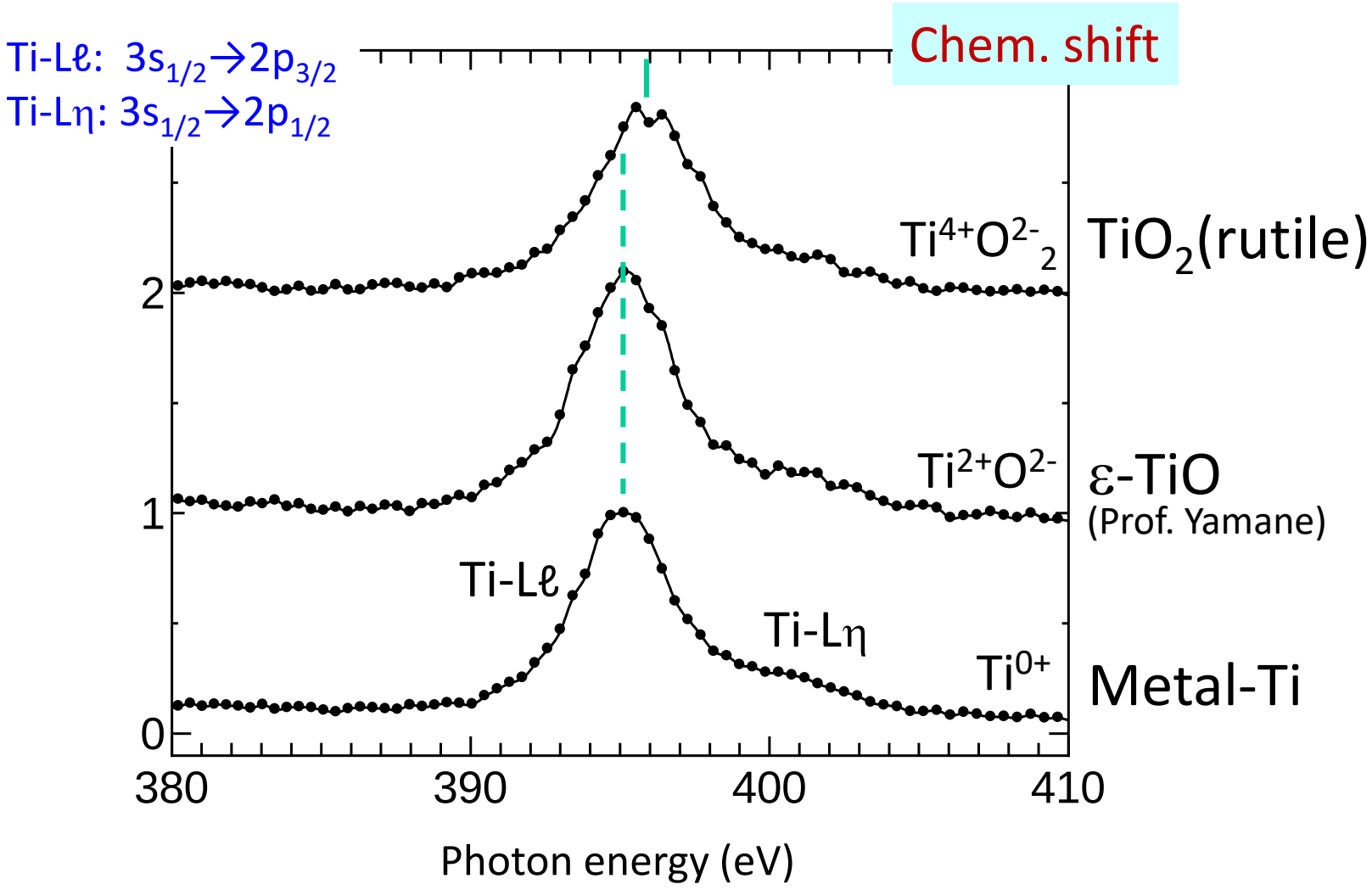

Chem. Shift: TiO +δ < TiO_2 ← tendency is consistent with XPS result

Discussion on chemical shifts in PES & XES

PES: Core→Vac. : $\Delta E^{F}_{B} = \Delta q/r - \Delta V - \Delta E_{R} - \Delta\phi$

ΔE^{F}_{B} : change of binding energy referred to Fermi level
$\Delta q/r$: core-level shift due to a change of valency
ΔV : solid state effect (crystal-field, DOS, Eg)
ΔE_{R}: relaxation effect (core-hole effect)
$\Delta\phi$: work function correction

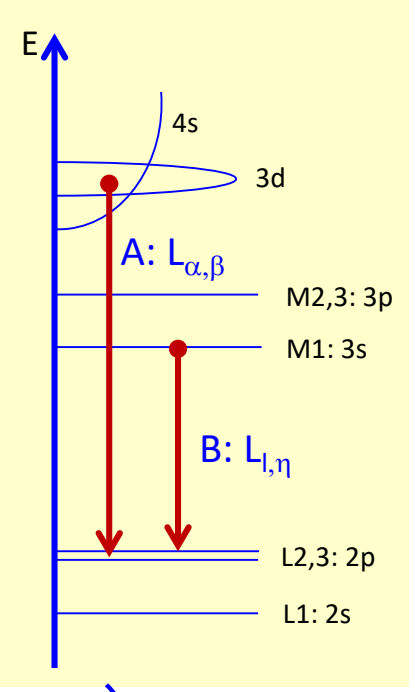

XES: VB→Core or Core→Core $\Rightarrow \Delta\phi = 0$

- VB→Core : no core-hole in final state $\Rightarrow \Delta E_{R} = 0$

$\Delta E_{B} = \Delta q/r - \Delta V$ ($L_{\alpha,\beta}$-emission)

- Core→Core : $(\Delta q/r)_{\Delta n,\Delta l}$ ~0 , ΔV ~0

$\Delta E_{B} = -\Delta E_{R}$ ($L_{\ell,\eta}$-emission)

Chemical shifts in $L_{\alpha,\beta}$ and $L_{\ell,\eta}$ emissions : different origins
(Lℓ shift: difference in core-potential screening by valence electrons)

M.Terauchi, *et al.*, *IOP Conf. Series Mater. Sci. Eng.* **304,** 012018 (2017).

Information of valency of 3d transition metal elements

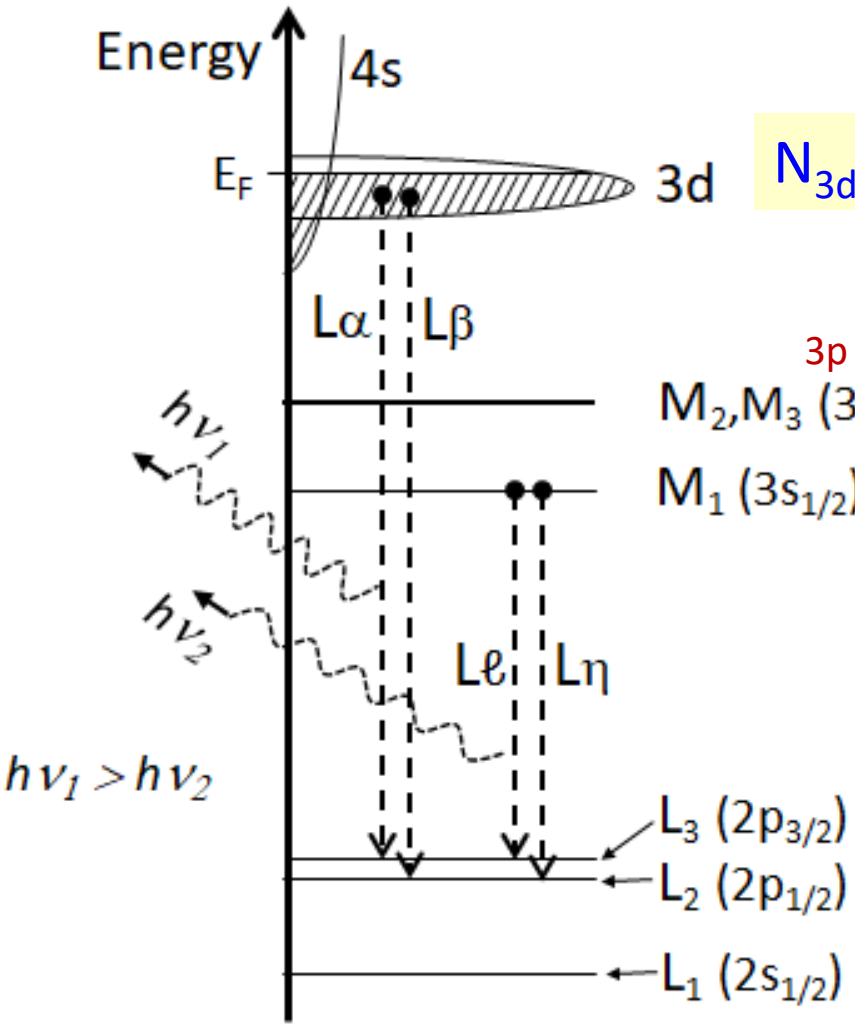

N_{3d}: variate form 1 to 10

3p cannot transit due to selection rule

N_{3S}: constant of 2

N_{3d}: can be reflected in intensity ration of Lα,β/Lℓ,η

Information of valence charge of 3d transition metal elements observed in L-emission spectra (MCP detector in PC mode)

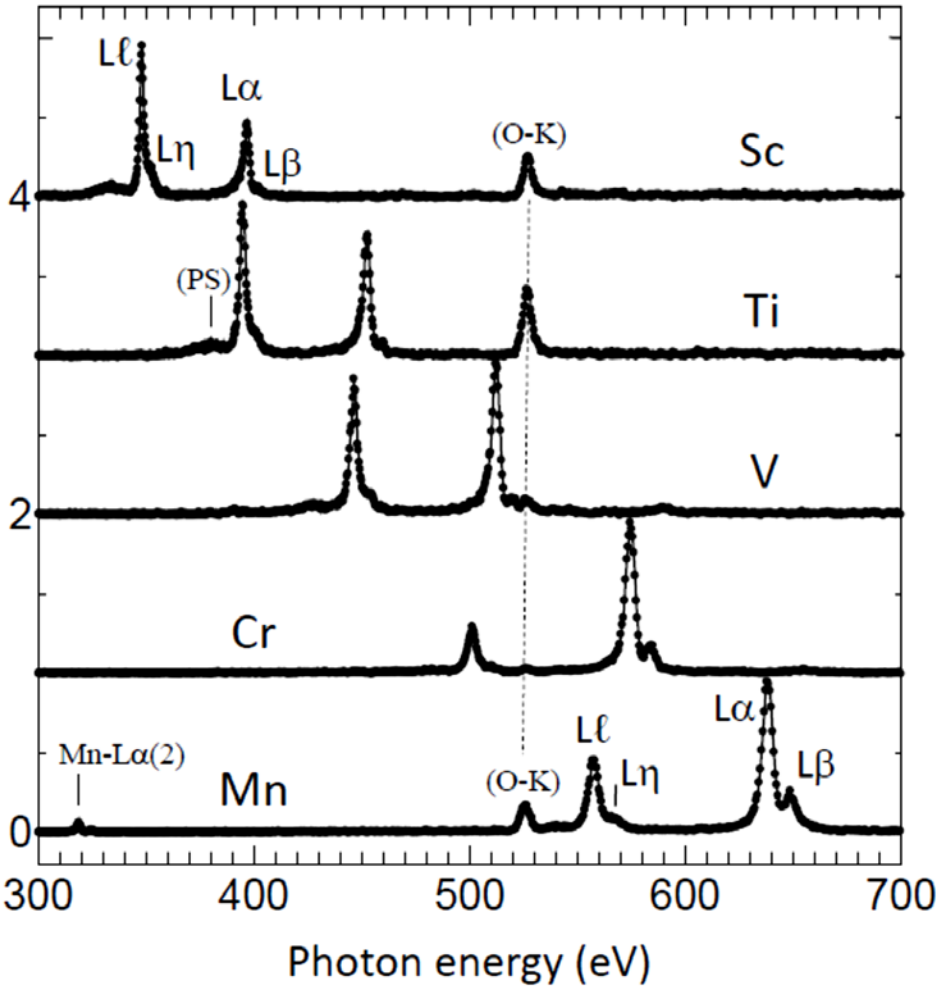

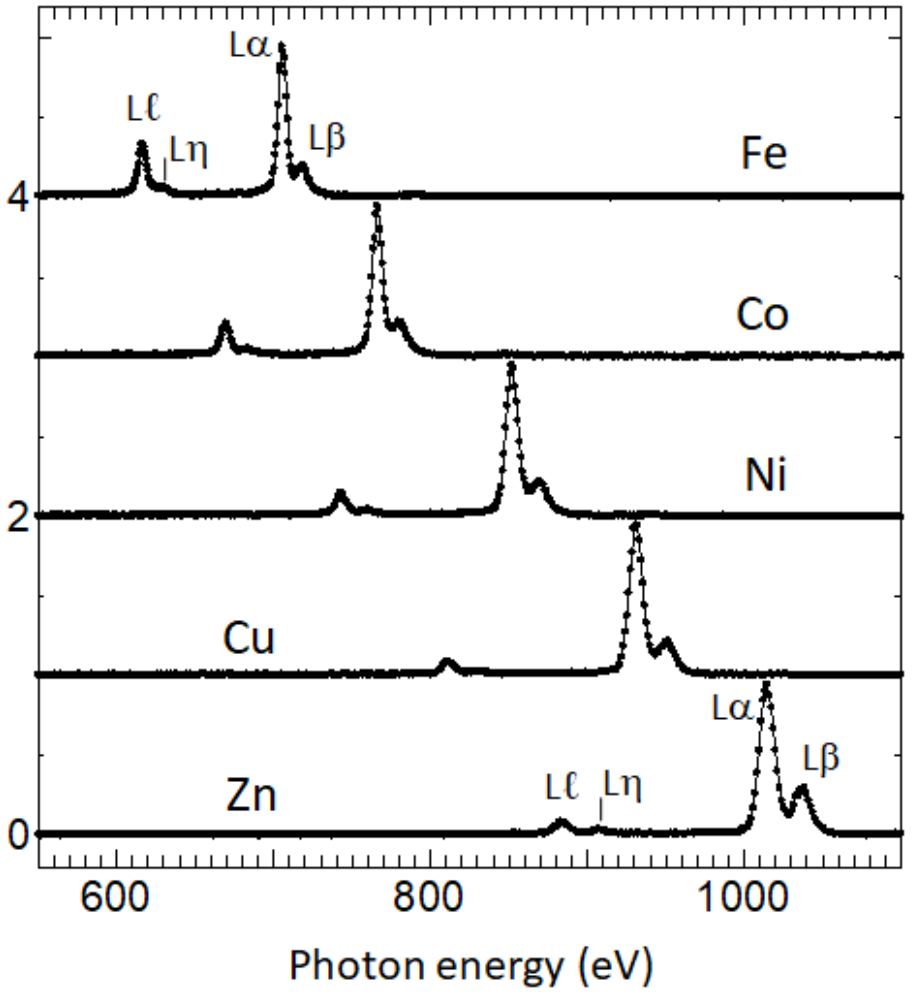

Lα,β/Lℓ,η gradually changes, except Cr.

Relation between N_{3d} and L-emission intensities

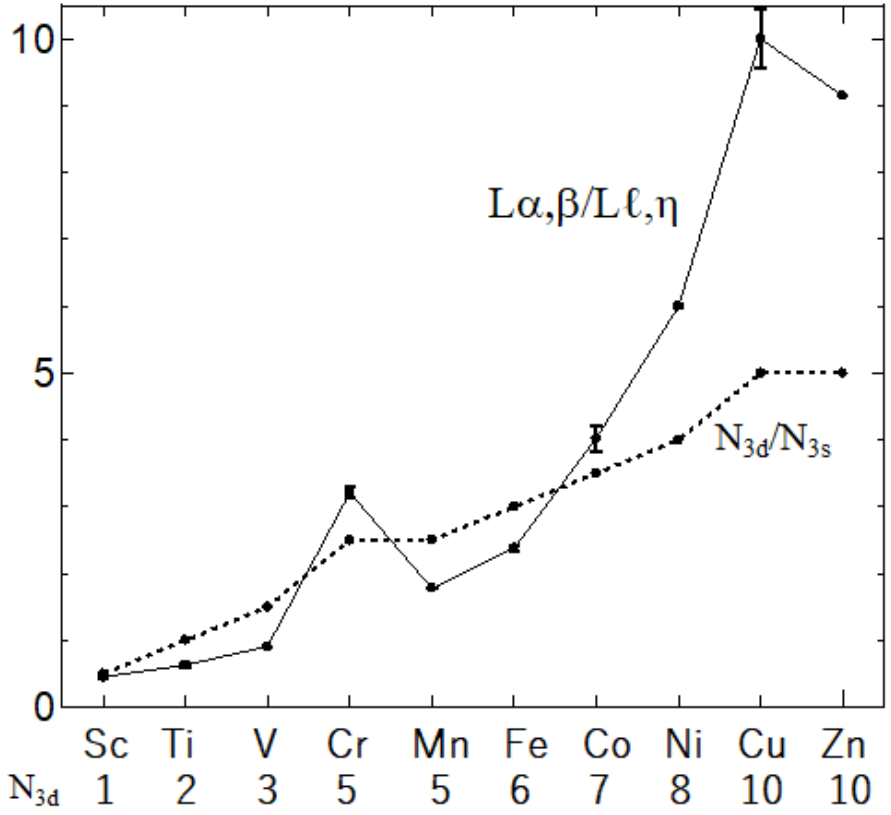

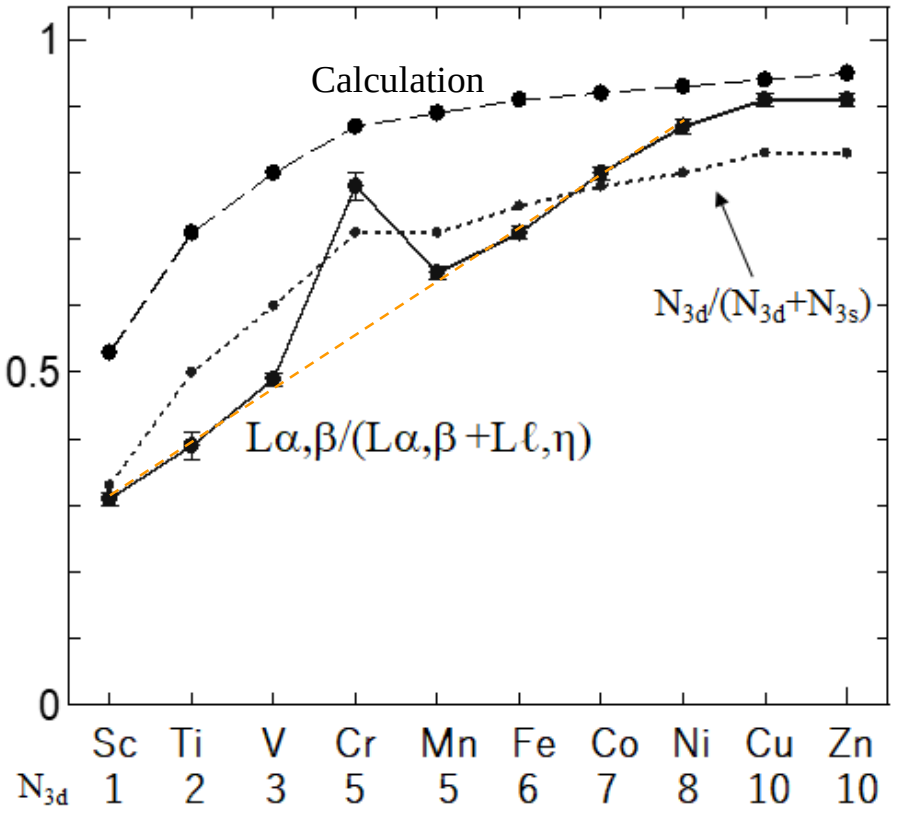

$L\alpha,\beta/(L\alpha,\beta+L\ell,\eta)$ changes almost linearly with N_{3d}

M.Terauchi, *Microscpyp* **68,** (2019), DOI: 10.1093/jmicro/dfz020.

4. SXES with mapping (EPMA)

a. *p*&*n* controlled MB_6 material
b. Amorphous CNx film

4a. MB_6 as a thermoelectric device materials

(Collaborated research with Prof. M.Takeda)

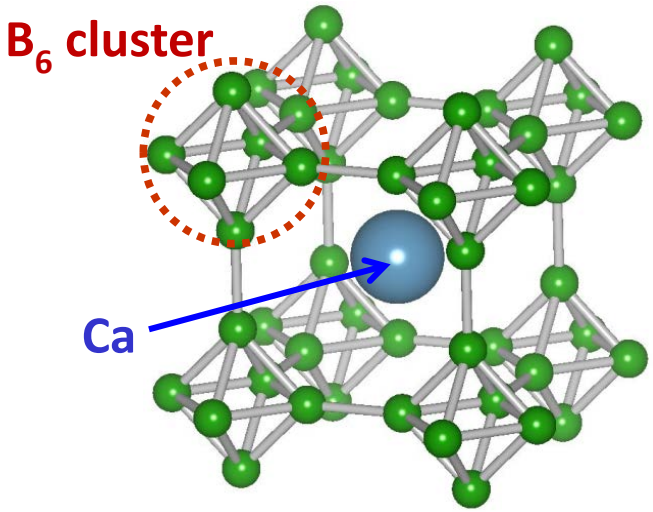

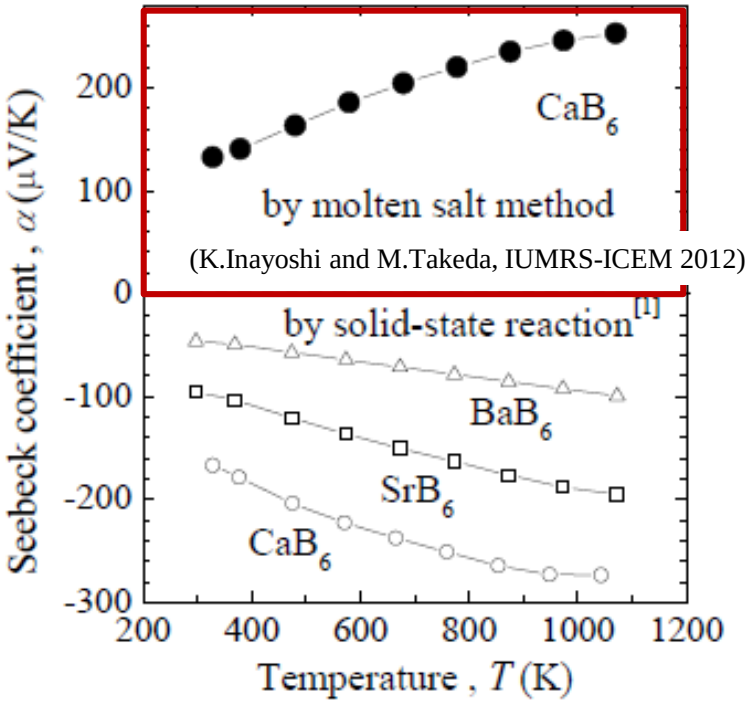

To be a device, *p*- & *n*-types are necessary.

/ CaB_6 by solid-state reaction
→ *n*-type semiconductor

/ CaB_6 by molten salt（Na_2BH_4+LiCl-KCl）method
→ *p*-type semiconductor
→ Na doped to Ca site (hole doping)
(DV-Xα calculation support it)

/ Recently, solid-state reaction with less Ca content → *p*-type semiconductor

DV-Xα

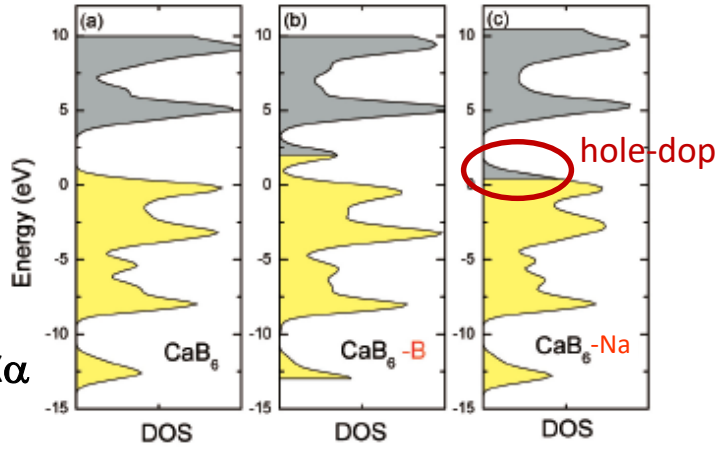

Evaluation by EPMA-SXES

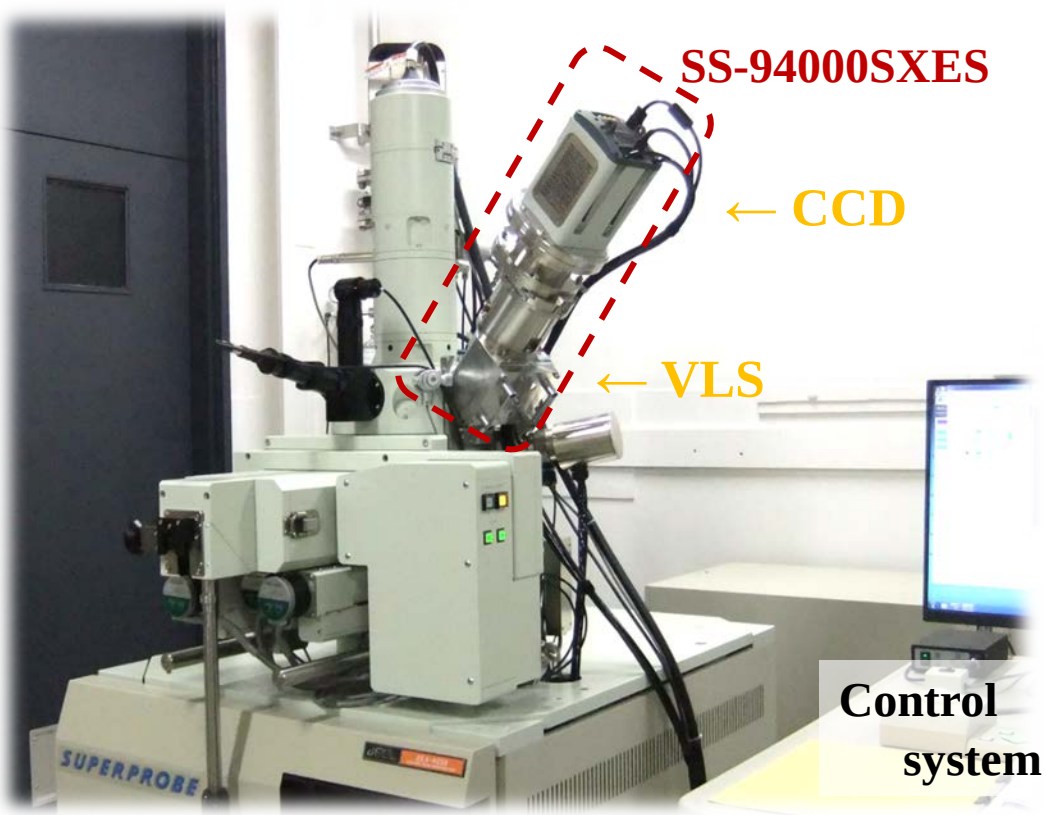

JXA-8230 with only SXES

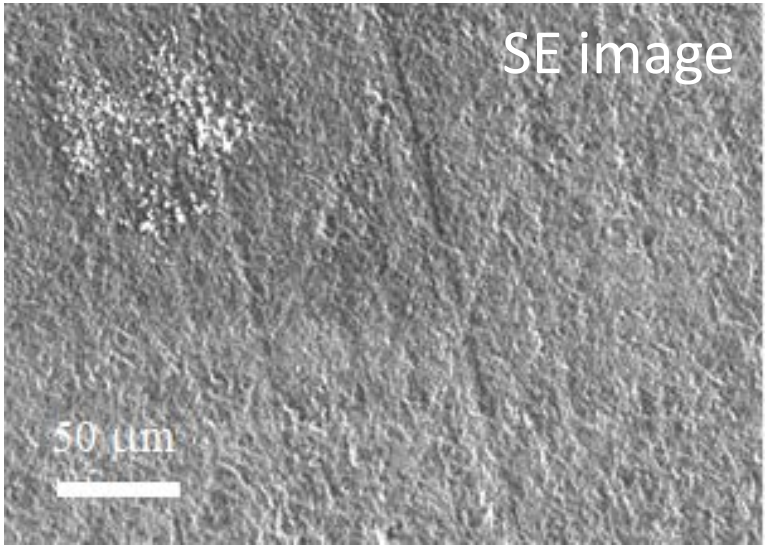

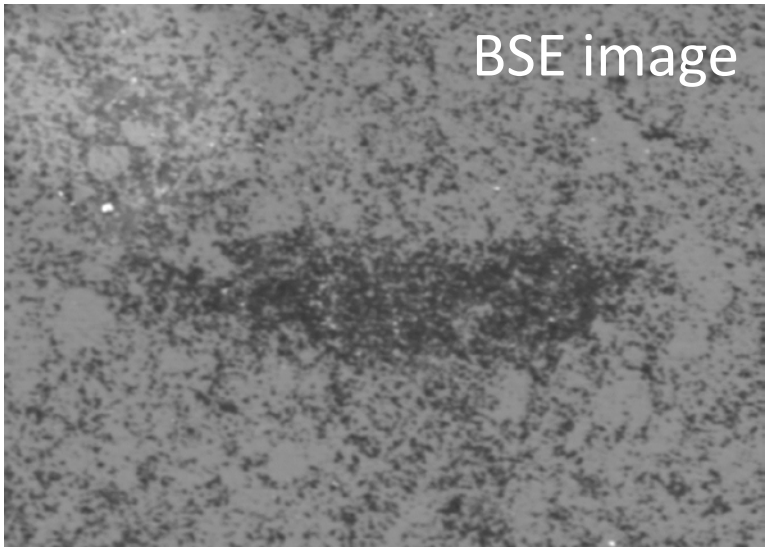

Bulk of Na-doped, *p*-type, CaB_6 →

M.Terauchi, *et al.*, *Microsc. Microanal.* **24(Suppl 1),** 746 (2018).

Images

Structure of CaB_6

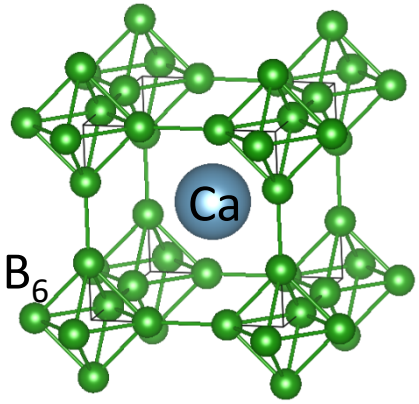

SE image

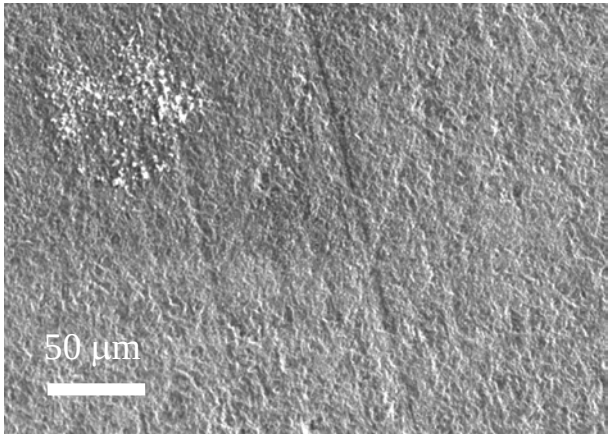

BSE image

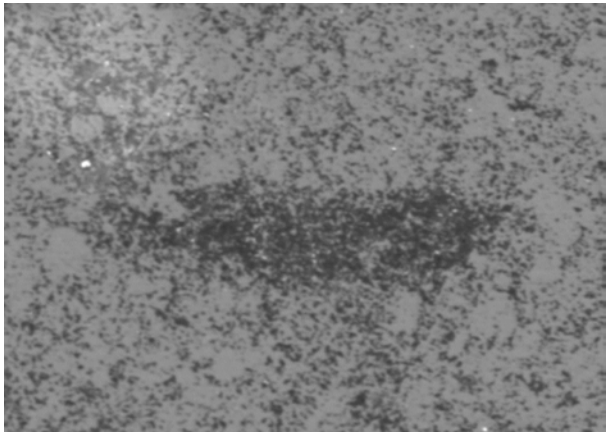

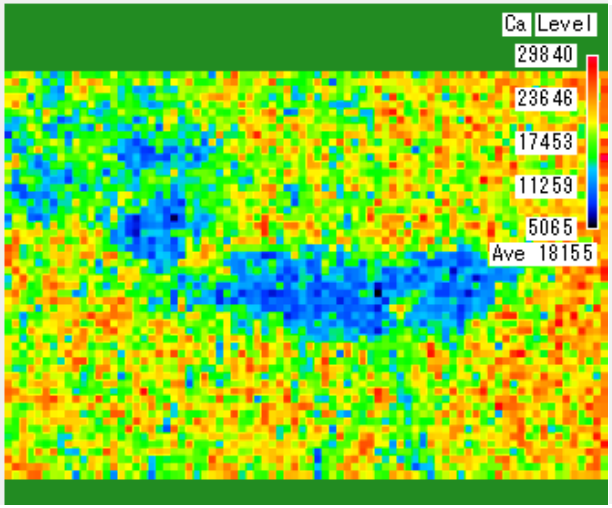

Ca-Ll,η image

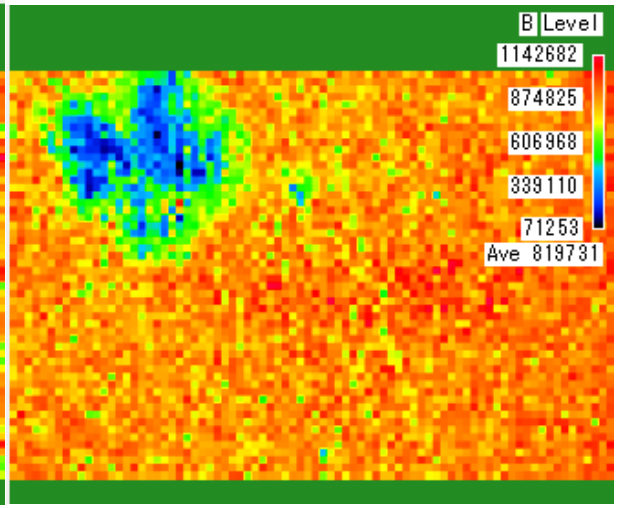

B-K image

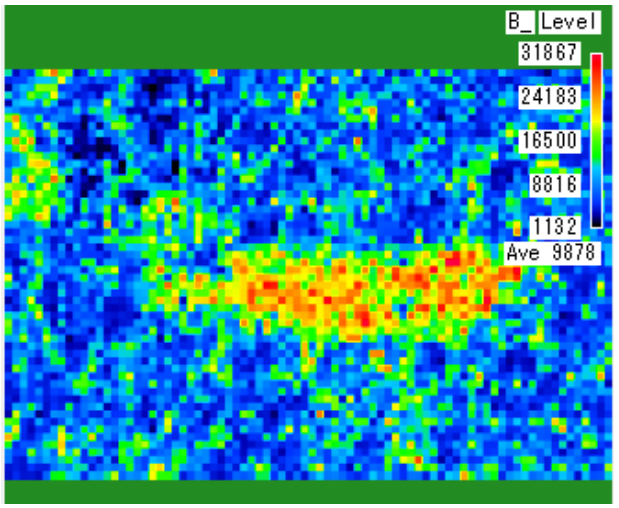

Top of B-K emission

Ca-deficient region has a difference in B-K spectrum

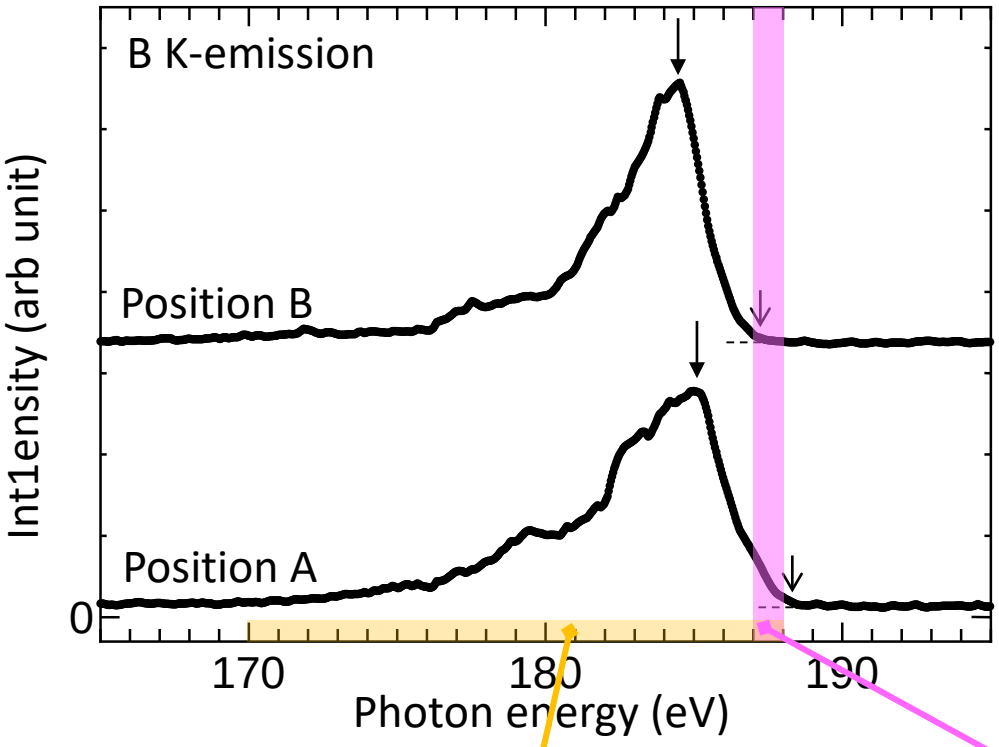

Mapping conditions
/ Acc. volt : 5 kV
/ Probe: 4μmϕ, 29 nA
/ 1 pix: 4x4 μm, 10sec
/ 80 x 54 pix → total 12 h

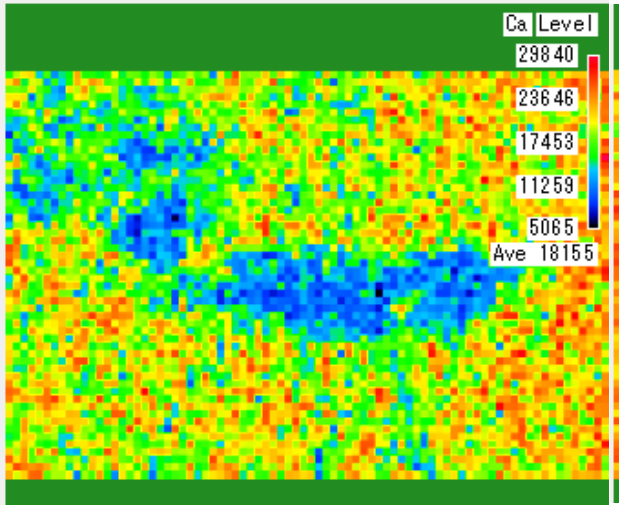

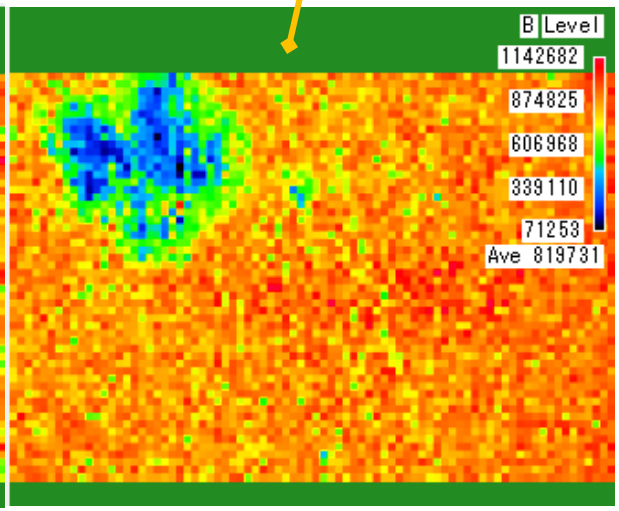

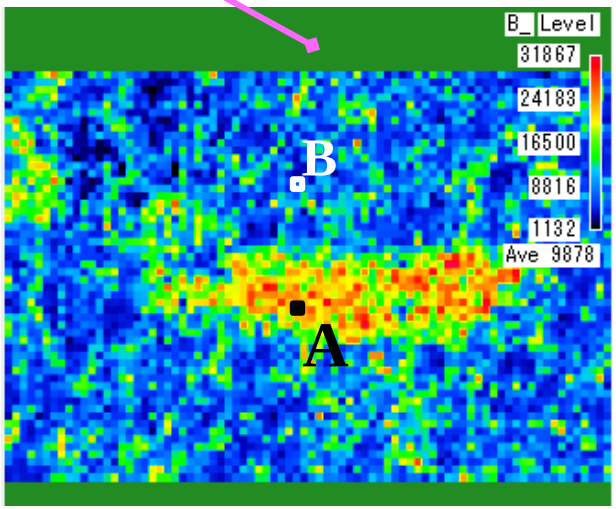

Ca-Ll,η image **B-K image** **Chemical image of B-K**

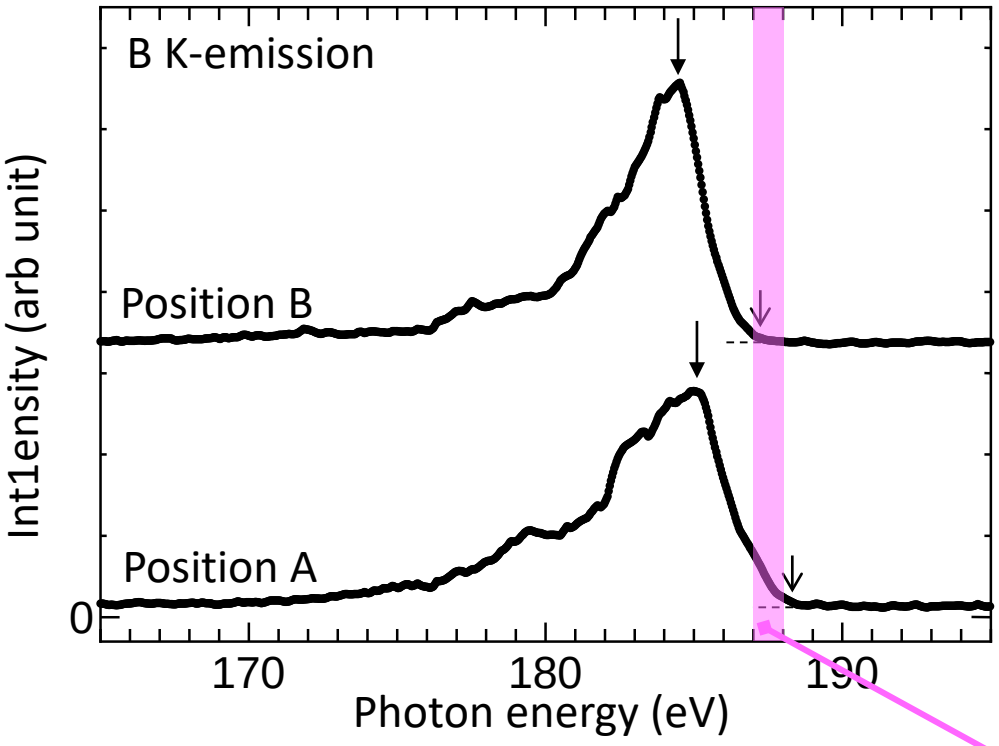

Mapping conditions
/ Acc. volt : 5 kV
/ Probe: 4μmϕ, 29 nA
/ 1 pix: 4x4 μm, 10sec
/ 80 x 54 pix → total **12 h**

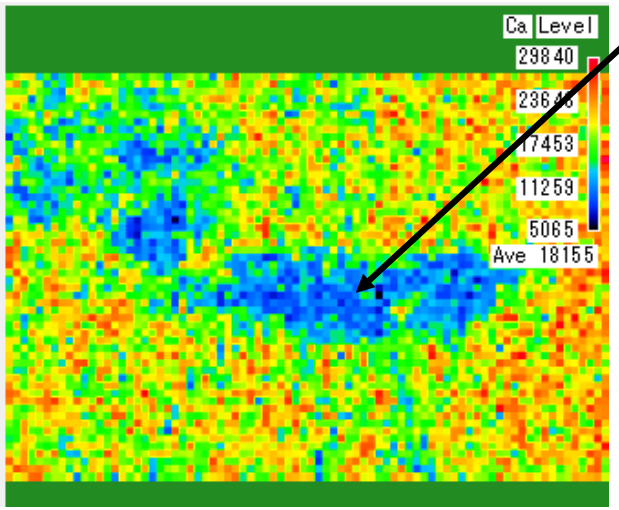

Ca-Ll,η image

Ca deficient (replaced by Na?, not confirmed)
→ Smaller charge transfer (hole doping)
→ Larger binding energy: 1s
→ **Chemical shift: +**
↓
Image of localized holes
(Similar to carrier doping in Si device.)

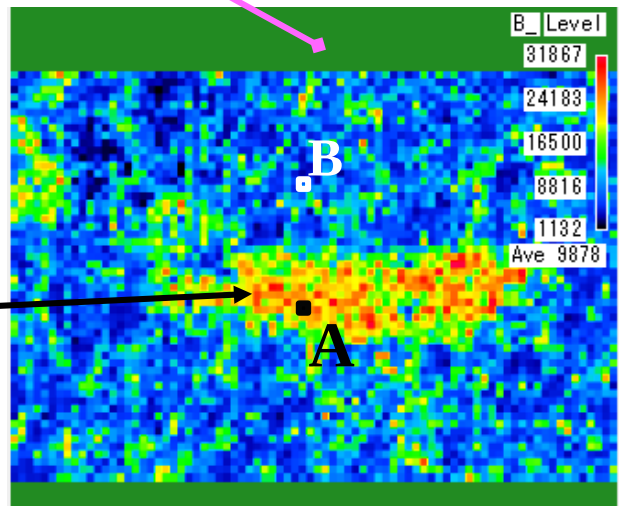

Chemical image of B-K

New preparation of p/n-controlled MB_6

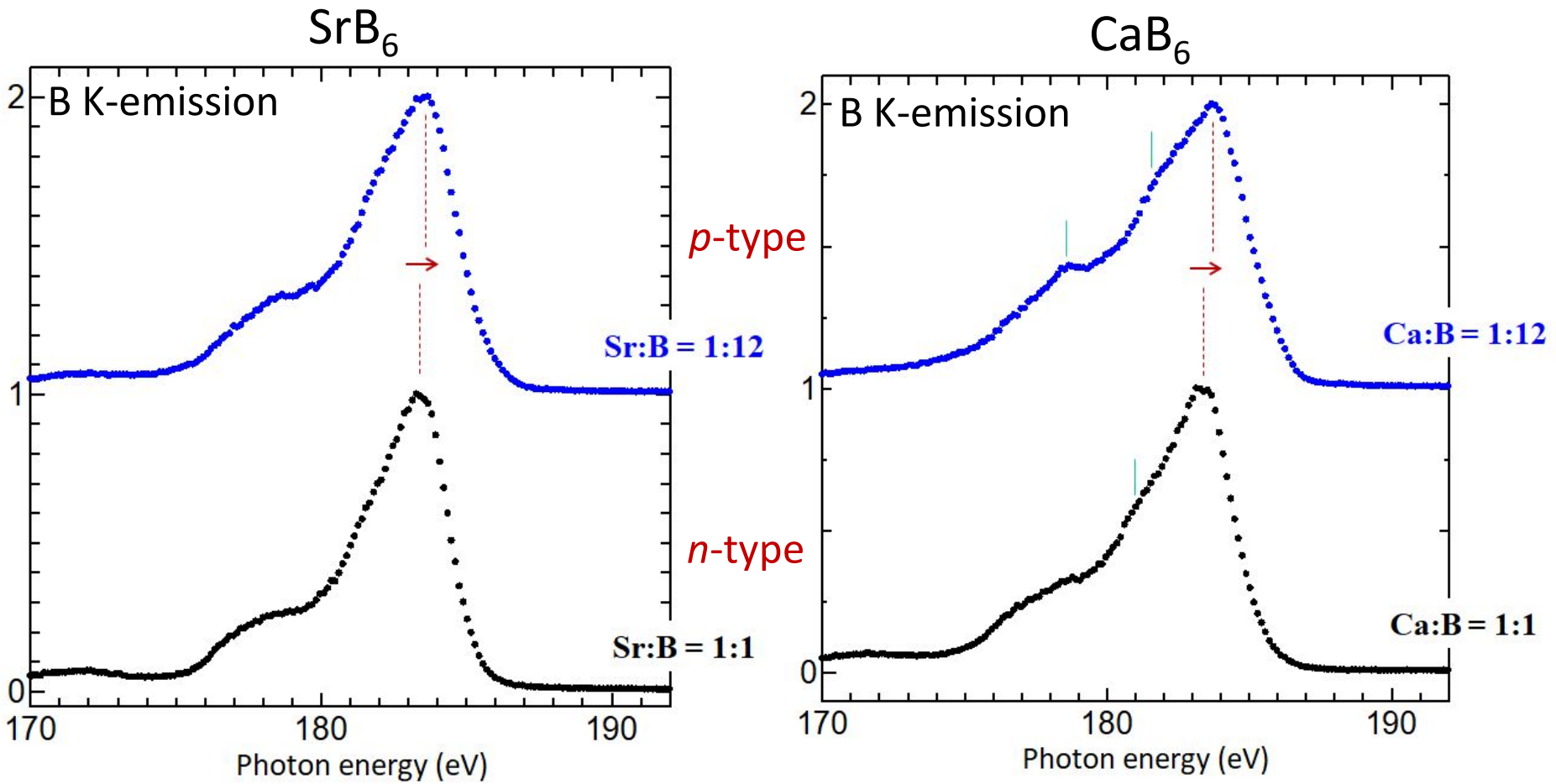

M deficient MB_6 indicates a hole-doping.⇒ How about the uniformity as a bulk？

Normal CaB_6: *n*-type

Ca-deficient CaB_6: *p*-type

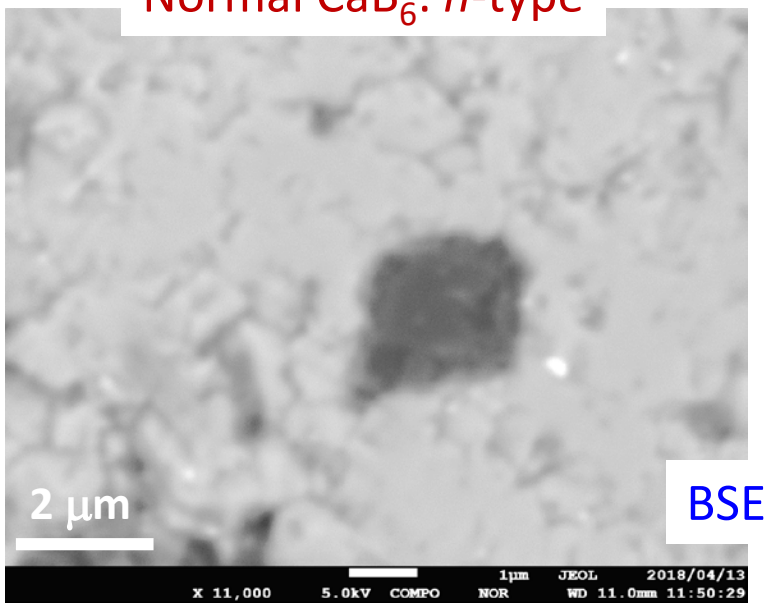

BSE image

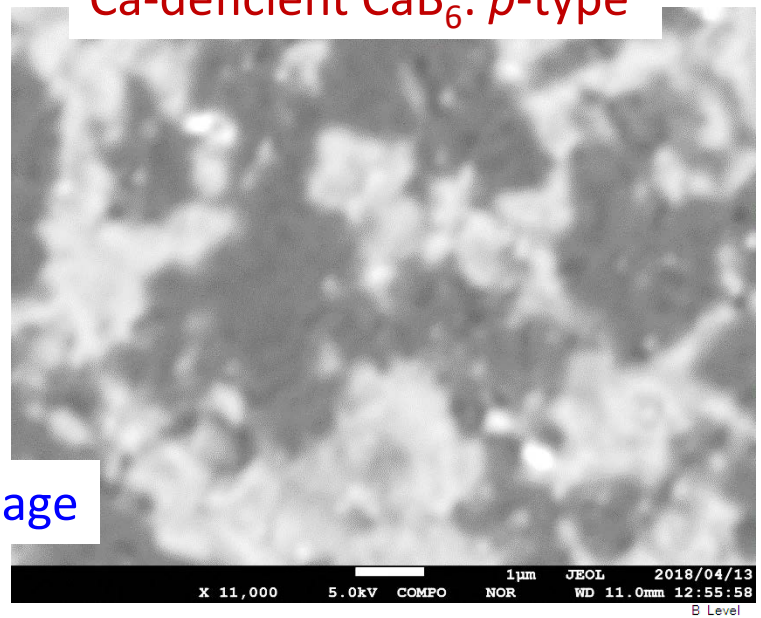

I_T / I_W
Chemical shift map

n-type

p-type

n-type

B 2 um

Separated into *p*- and *n*- domains?

4b. Amorphous carbon nitride (a-CNx) film

（Collaborated research with Prof. M.Aono）

【Character】
- Optical conductivity
- Optical deformation
- Visible light emission

【Application】
- Optoelectronic device
- Light Emitter
- Light-sensitive device

etc...

【Key issue】

Control of resistivity

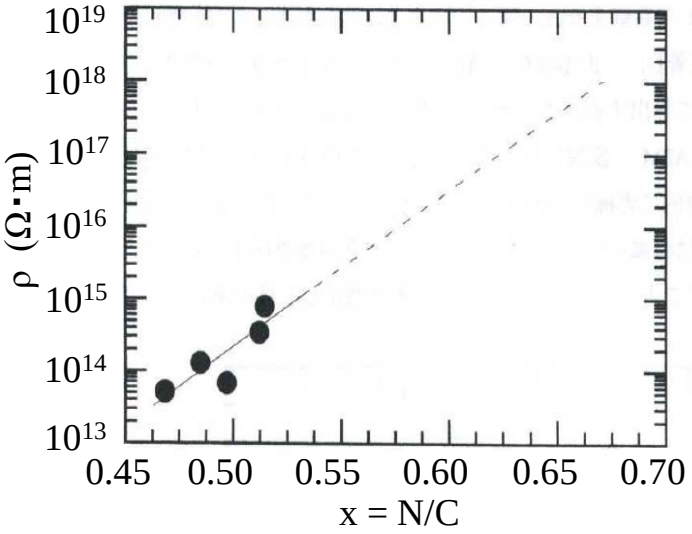

（ S.Nitta et al.,応用物理, 69, 782 (2000). ）

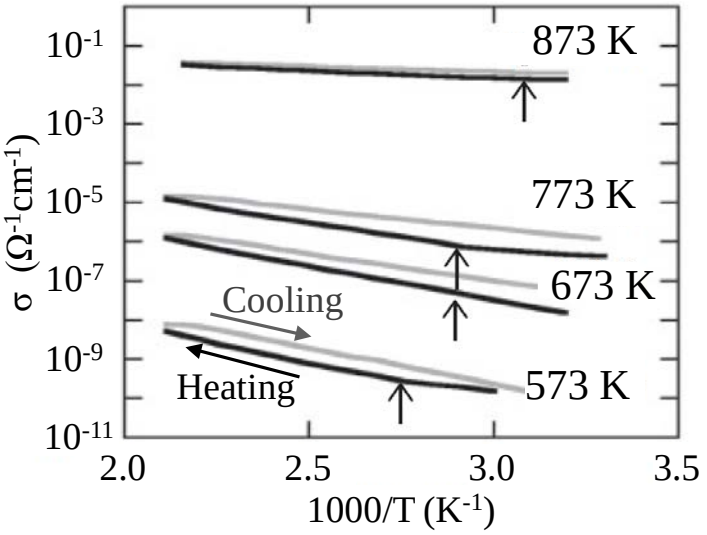

（ N.Tamura, *et.al.*, JJAP, 53, 11RA09 (2014). ）.

Relation between x & ρ ? and T_{deop} & σ(1/ρ) ?

Specimens

【Preparation】
- Magnetron sputtering: formed on Si wafer
- Target: Graphite (99.99%)
- Reactive gas : N_2 (99.9999%)

【Macroscopic character】

(T_{depo} : low ⇒ x : large ⇔ ρ : large)

	T_{depo}	x	ρ	t
1	200 ℃	0.52	6.4×10^7 Ω・m	813 nm
2	400 ℃	0.41	2.3×10^5 Ω・m	934 nm
3	500 ℃	0.40	3.4×10^2 Ω・m	935 nm

・TEM observation

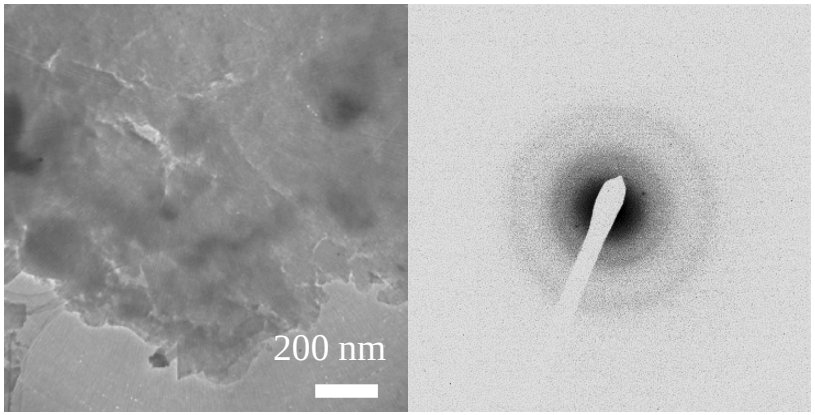

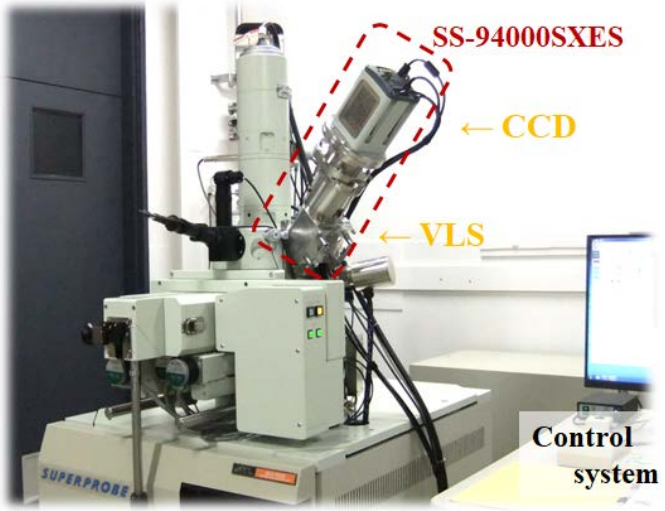

SXES spectrum of a-CNx: EPMA-SXES@5kV

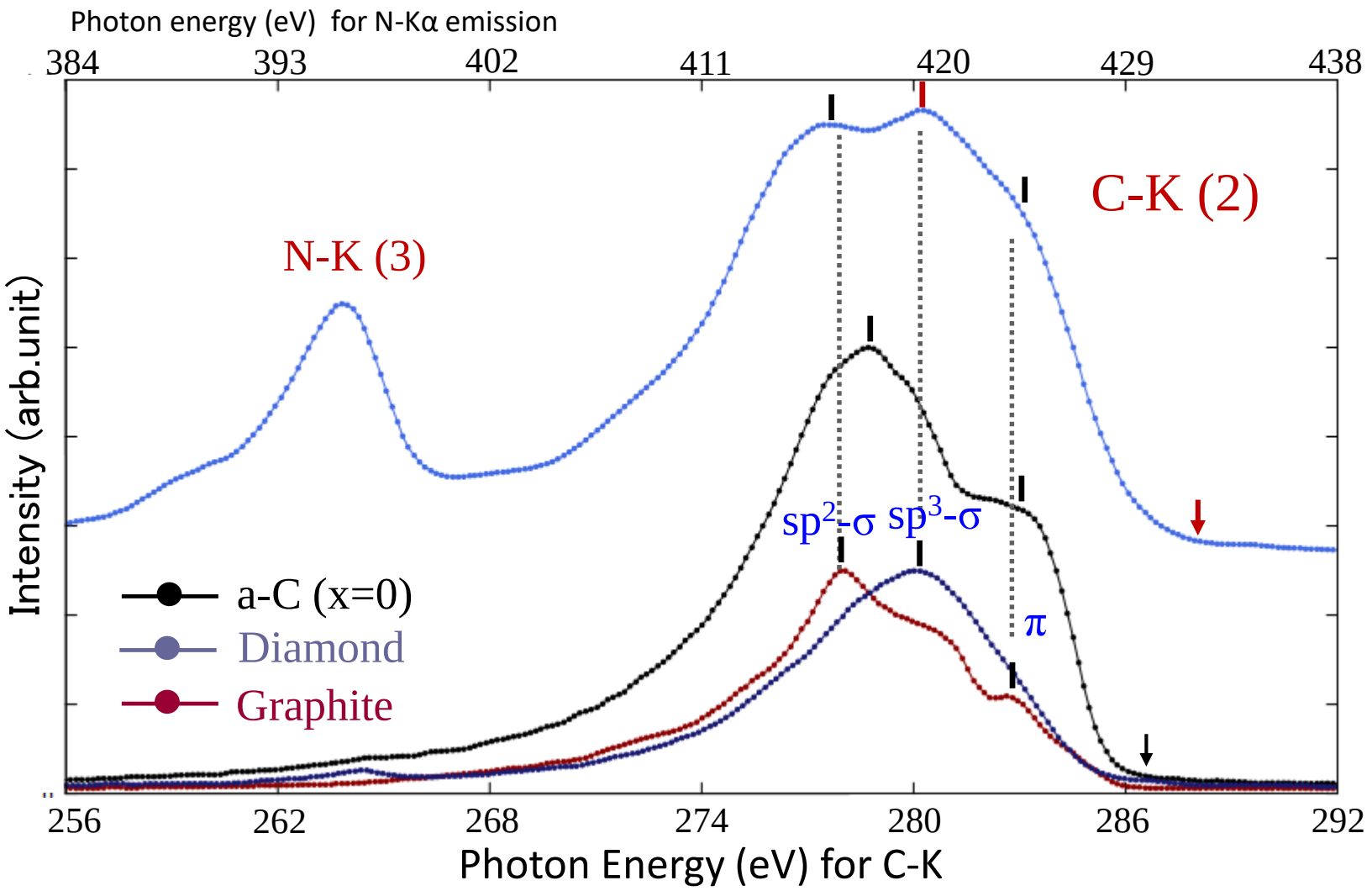

a-CNx: **intensities at sp^3-σ and VB_{top} increase**

SXES spectra for different x

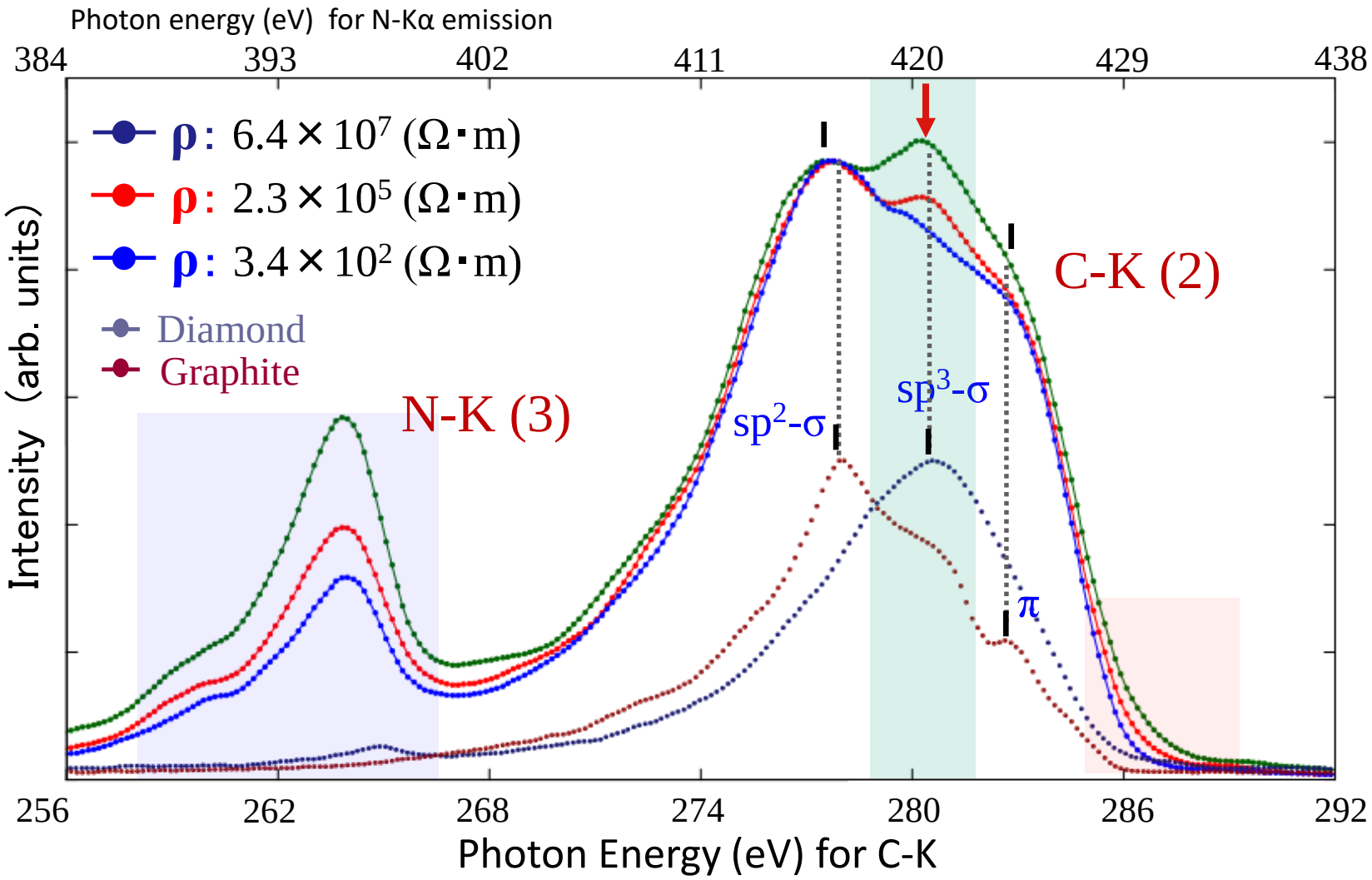

ρ: large ⇔ x: large ⇔ sp^3-σ, VB-top

Spectral mapping of a-CNx

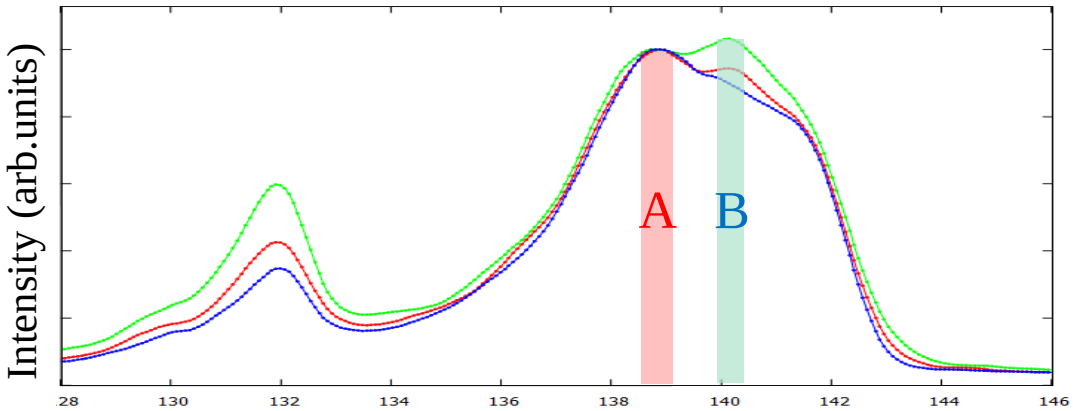

① ρ: 3.4×10^2 (Ω･m)

② ρ: 2.3×10^5 (Ω･m)

③ ρ: 6.4×10^7 (Ω･m)

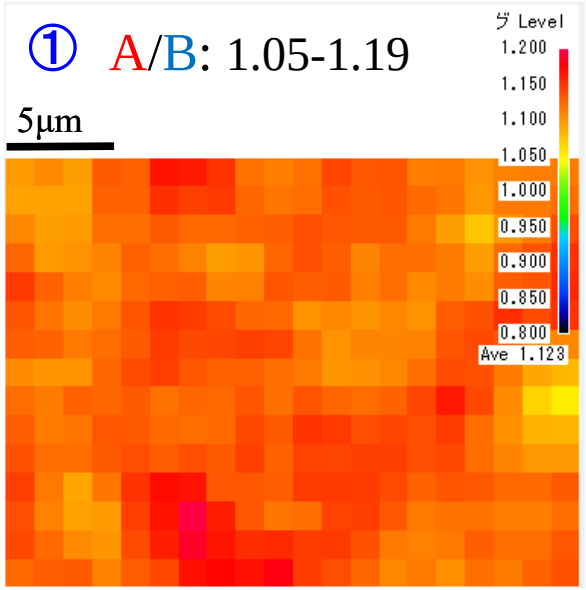

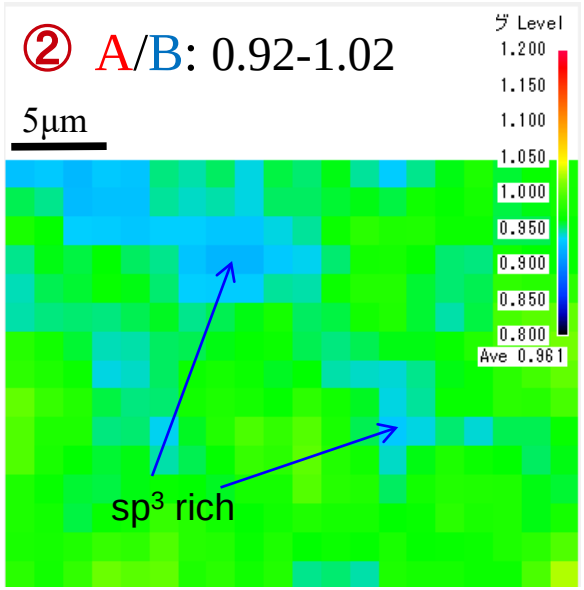

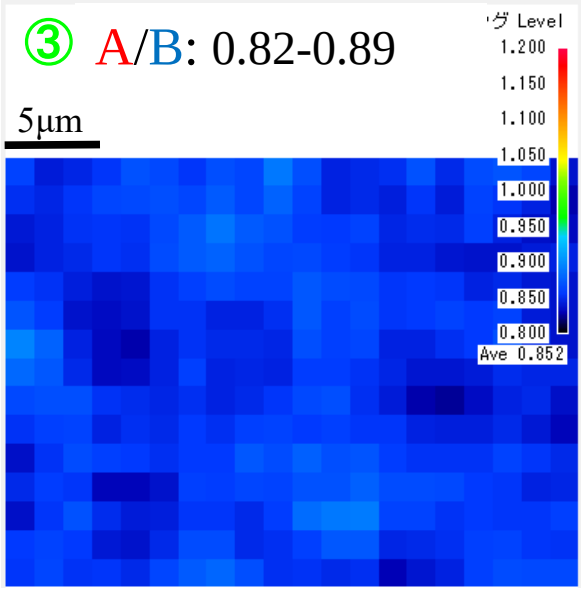

Fluctuation of A/B in film < 10%

S.Ishii, *et al.*, *Microscopy* **67,** 244 (2017).

Optical deformation of a-CNx and bonding

Figure 1. Typical photomechanical response of a-CN_x film. The substrate is a 12-μm thick poly(ethylenenaphthalate) film.

SEM-SXES-Laser →

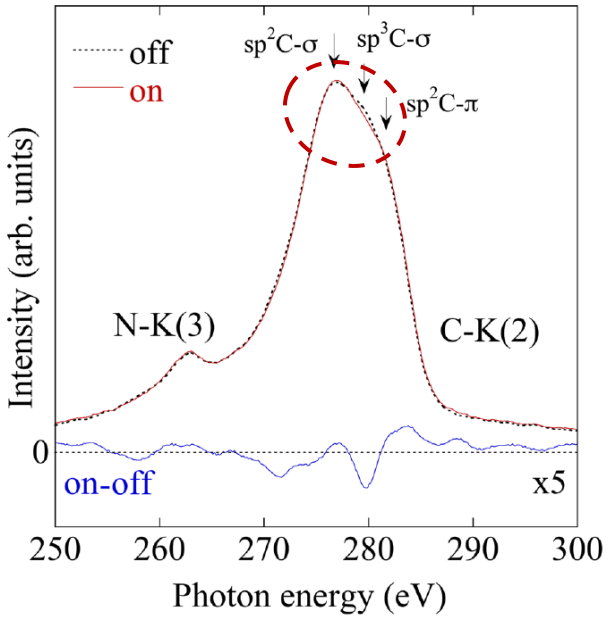

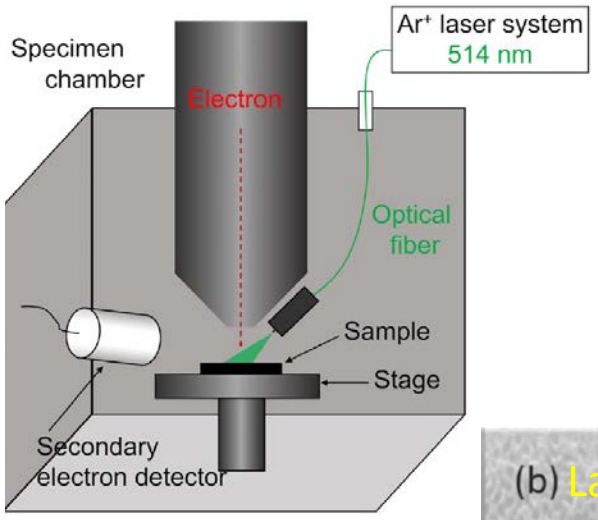

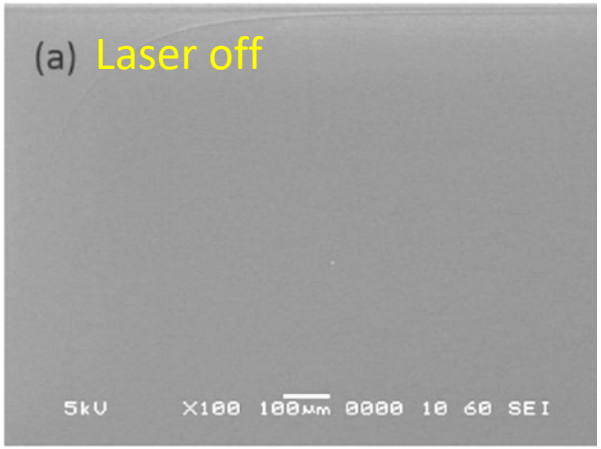

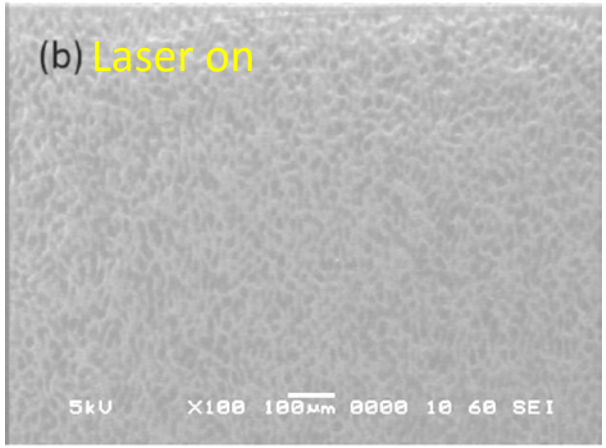

M.Aono, *et al.*, *Scientific Reports* **8,** 15066 (2018).

5. Improvements in SXES electron microscopy

a. Reflection efficiency of VLS grating
b. Energy resolution
c. Energy calibration

5a. A try to improve detection efficiency

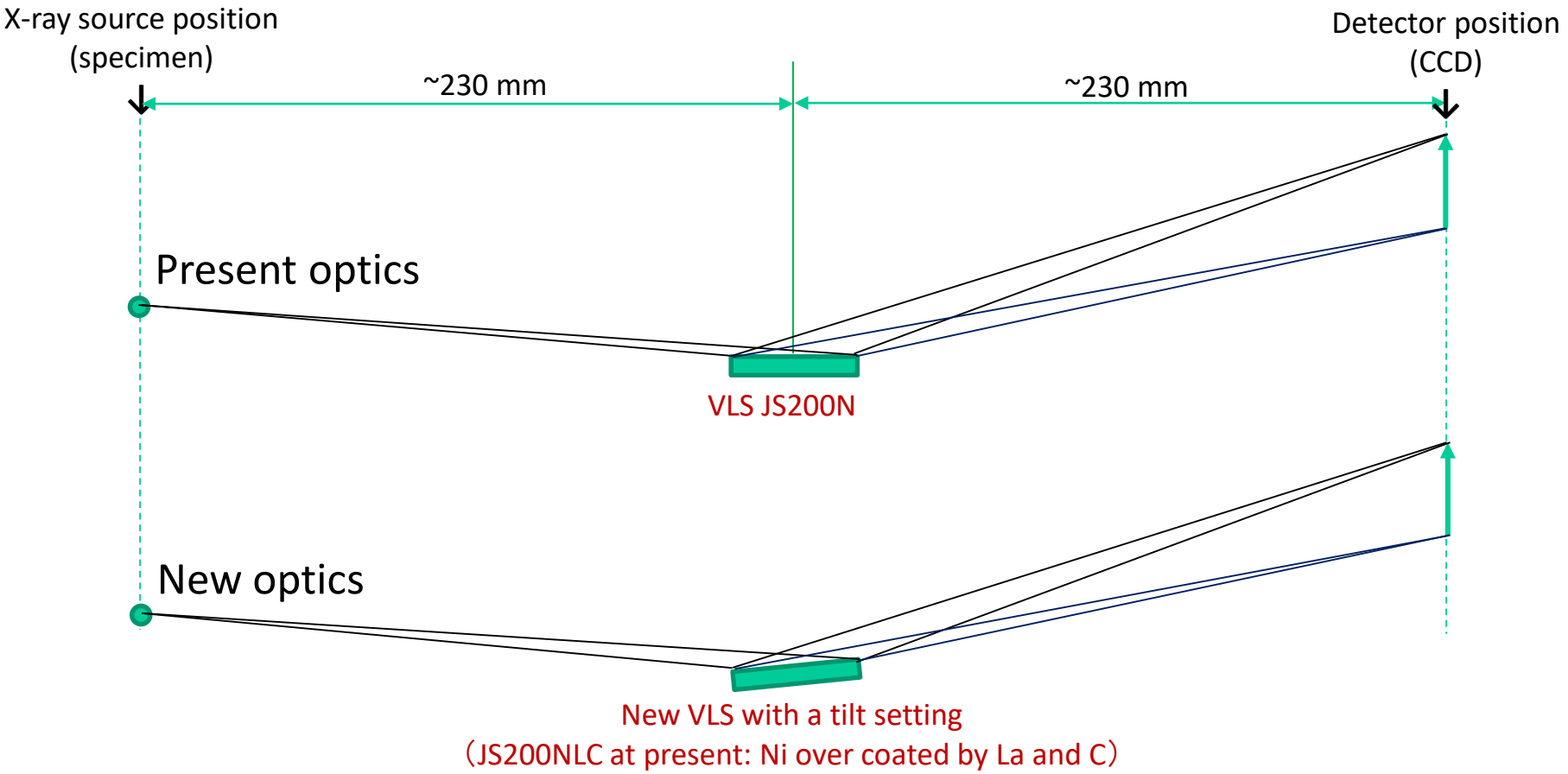

/ larger solid angle by a tilt of a VLS grating
/ larger reflectivity by an additional coating

A test result by SEM-SXES@Tohoku

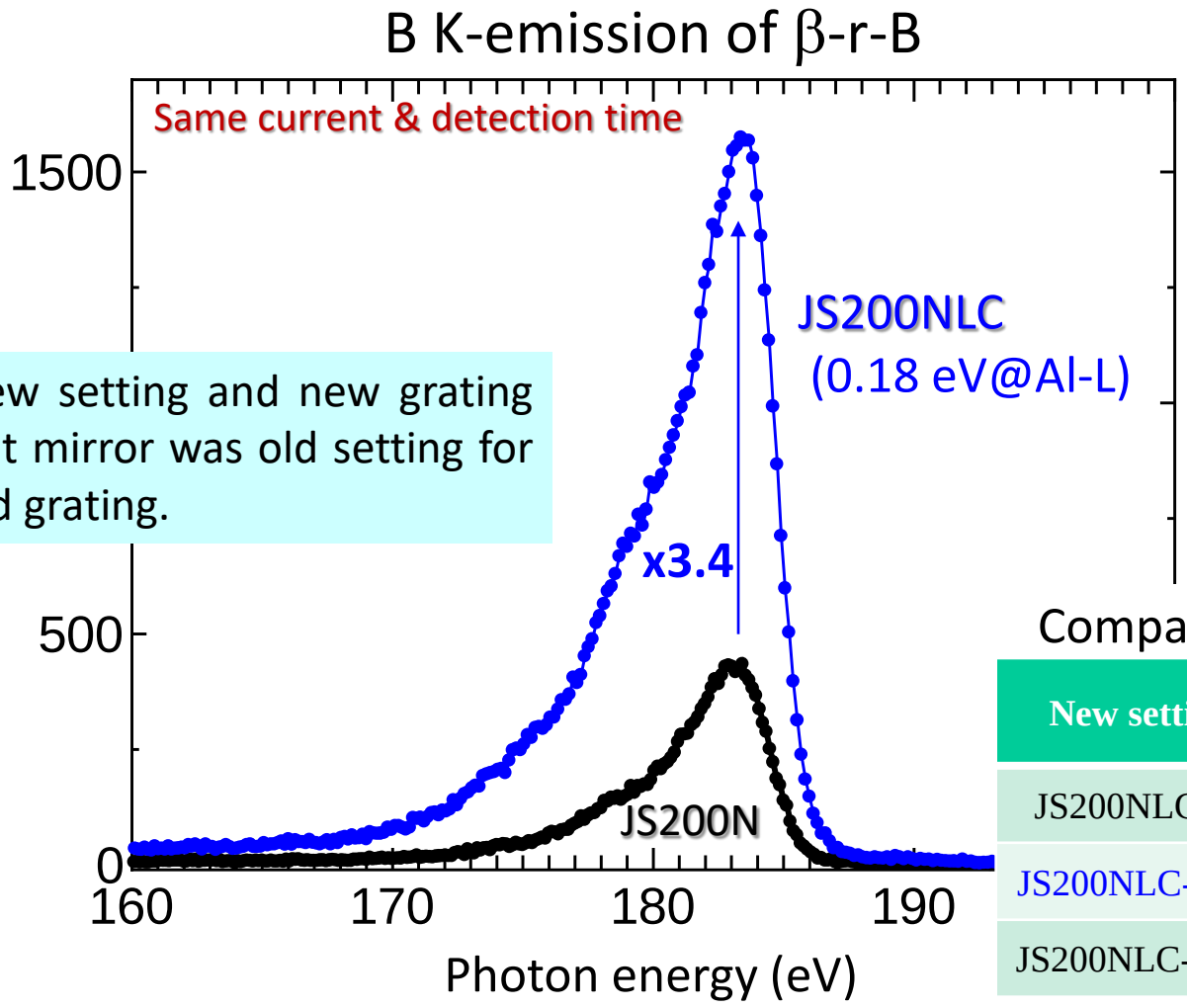

New setting and new grating but mirror was old setting for old grating.

Comparison of reflectivity only

New setting	B-K 1st	Include solid angle improve
JS200NLC-Ni	x1.0	x2.0
JS200NLC-LaF_3	x2.1	x4.2
JS200NLC-La/C	x2.5	x5.0

New problem: BG is not smooth → Fitted subtraction is necessary

5b. A try to improve energy resolution

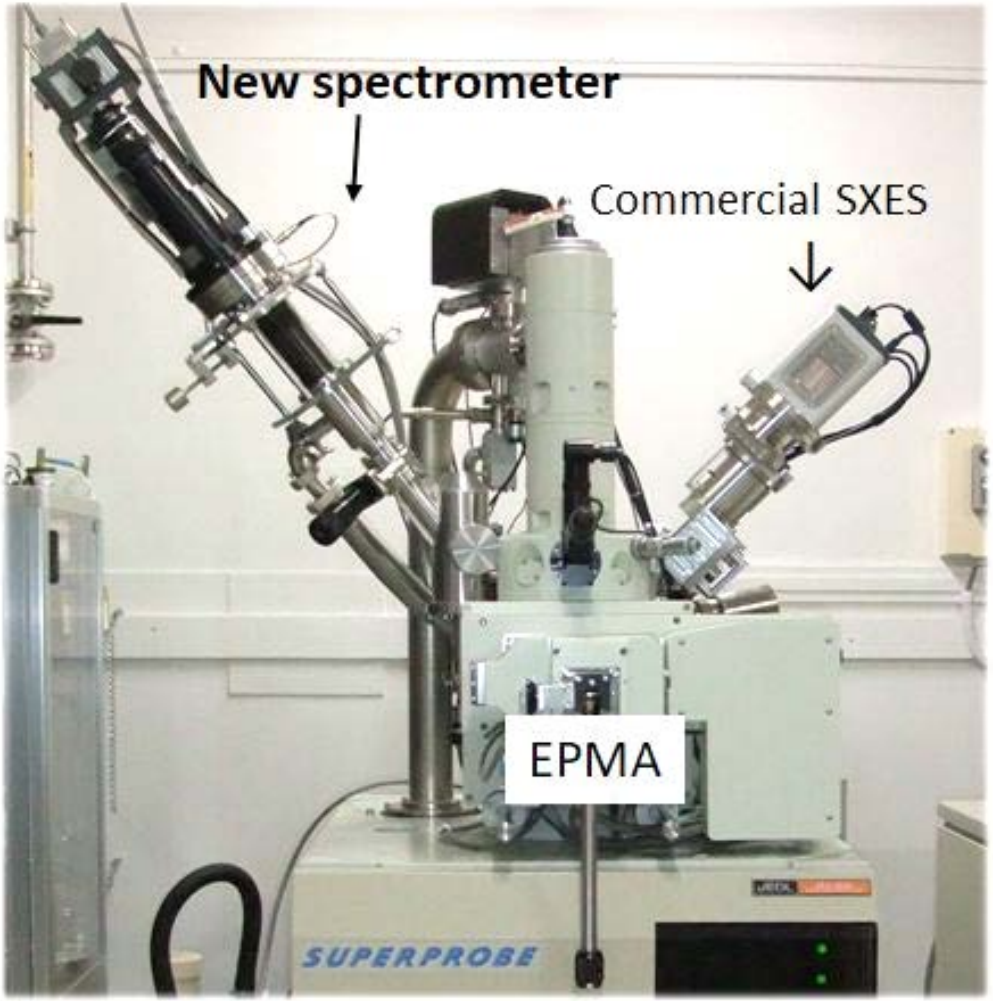

・VLS grating ~ detector: x 2, Normal MCP detector

Aim: search an effectiveness of an improvement in energy resolution

A test result of B K-emission of LaB_6

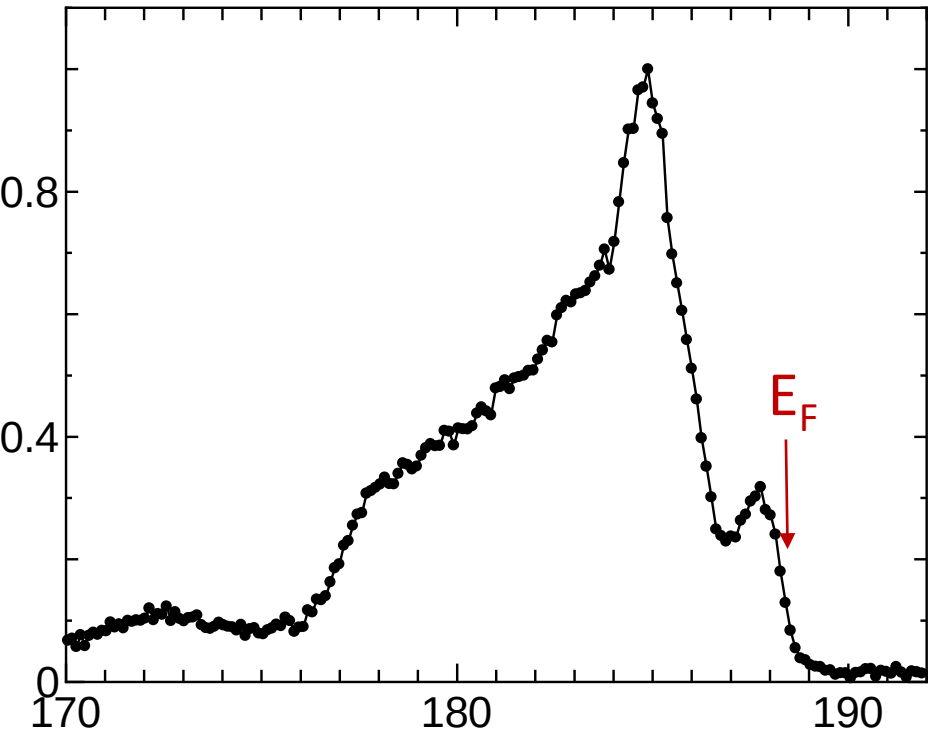

Photon energy (eV)

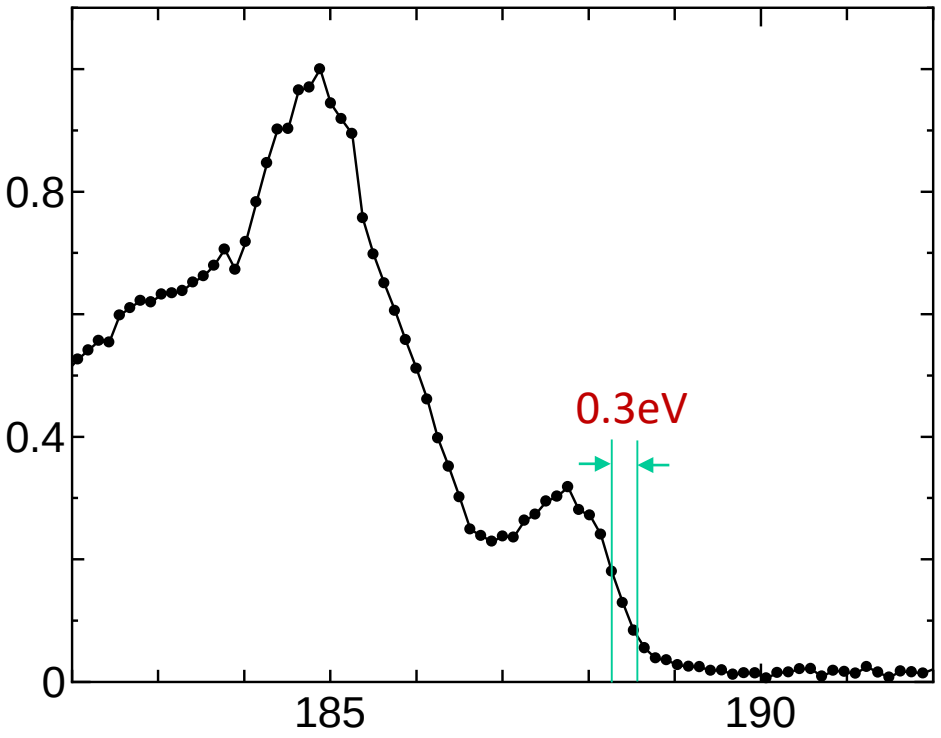

Photon energy (eV)

$E/\Delta E$~620

5c. A try to improve energy calibration

Element	Kα_1	Kα_2	Kβ_1
3 Li	54.3		
4 Be	108.5		
5 B	183.3	(185.2)	
6 C	277	(277.0±2.0)	
7 N	392.4		
8 O	524.9		
9 F	676.8		
10 Ne	848.6	848.6	
11 Na	1,040.98	1,040.98	1,071.1
12 Mg	1,253.60	1,253.60	1,302.2
13 Al	1,486.70	1,486.27	1,557.45
14 Si	1,739.98	1,739.38	1,835.94

Orientation dependence

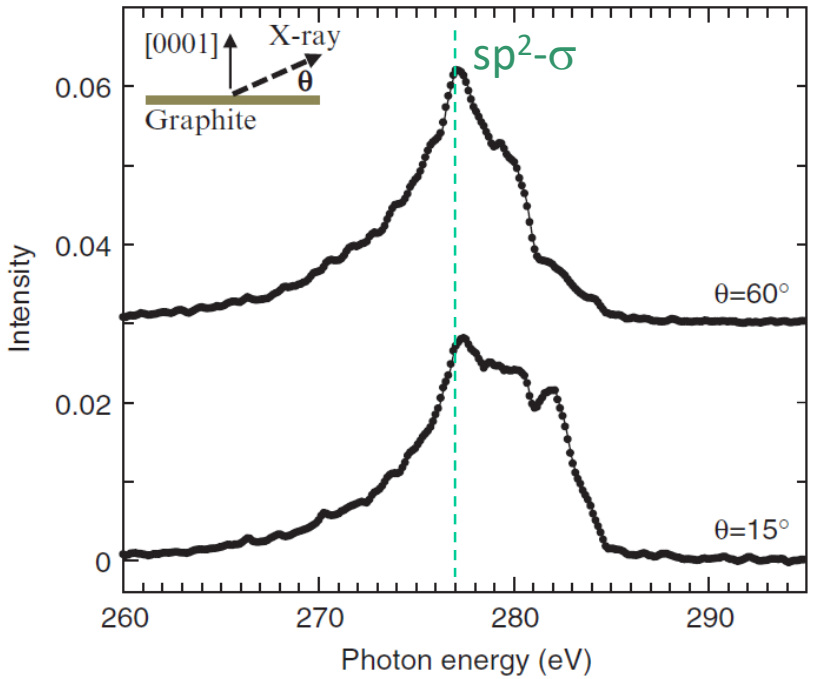

/ C K-emission (graphite sp^2-σ) peak is sharp and convenient to energy calibration.
However, accuracy of C K-emission energy in table is not enough.
/ B K-emission energy is reported in two values.

⇒ C-K (graphite sp^2-σ peak) and B-K (β-r-B) are calibrated
by using Sc Lα(2), Lα(3), Lℓ(2), Lℓ(3), and Al-L.

(Bearden, Rev. Mod. Phys. 39, 78 (1967), Sc-Lα:395.4eV, Lℓ:348.3eV)

C-K emission spectra of graphite and diamond

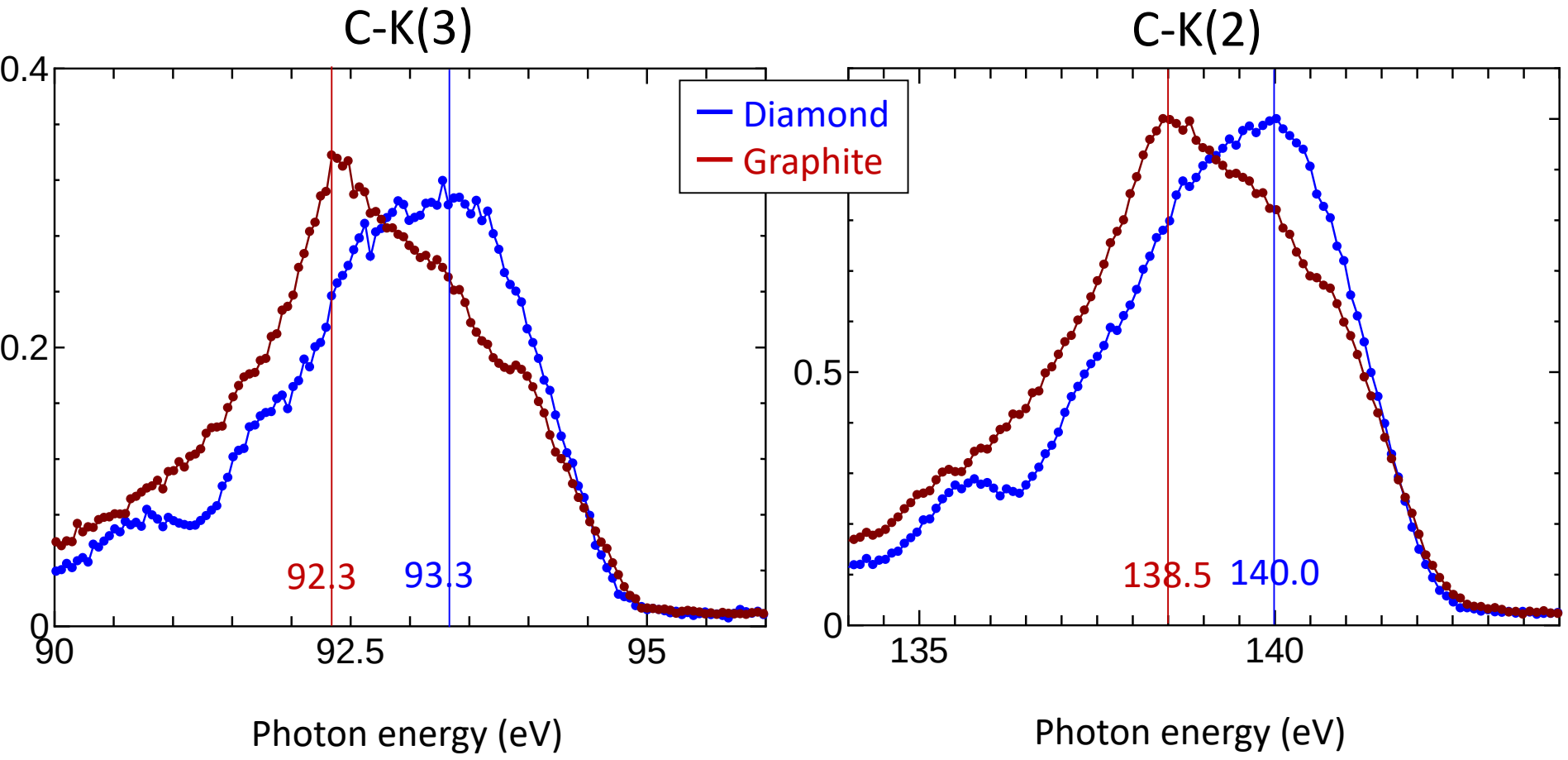

Graphite sp^2-σ: 277.0 eV / Diamond sp^3-σ: 278.0 eV

B K-emission peak energy of β-r-Boron

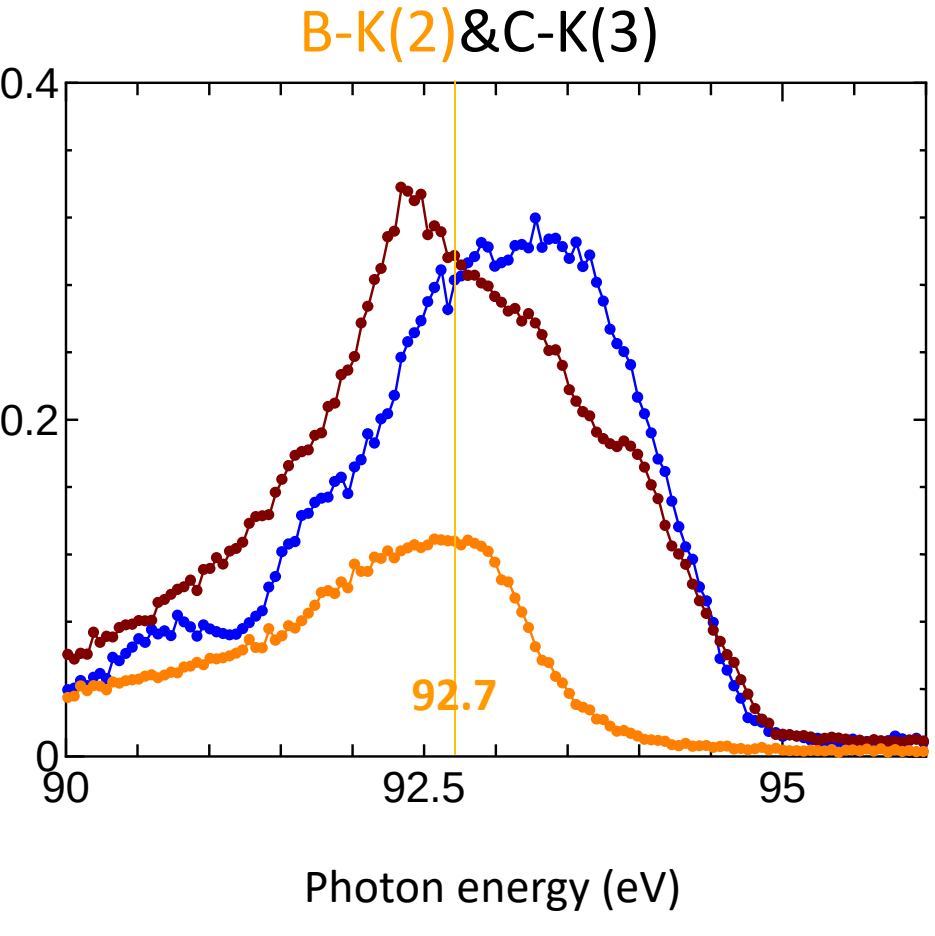

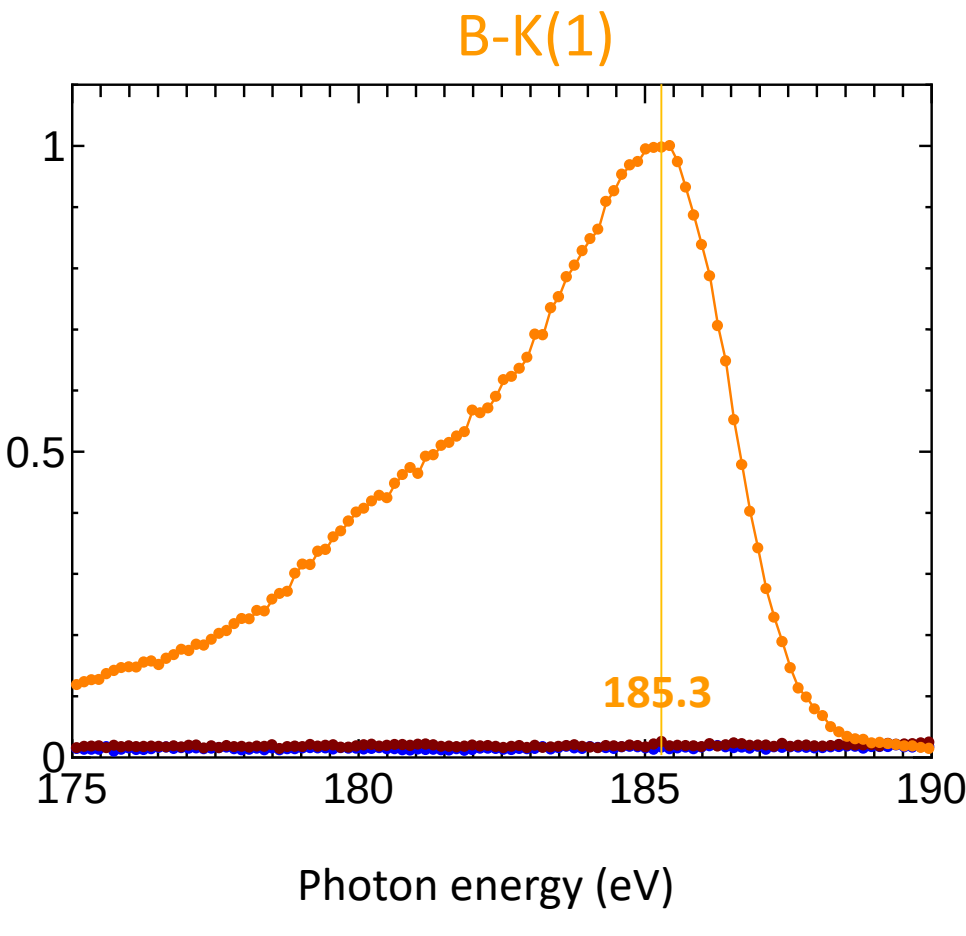

β-r-Boron: 185.3 eV

Summary

SXES profile informs the energy state of bonding states which is the origin of physical properties of materials.

1. 3d TM element: N_{3d} reflects in $I(L_{\alpha,\beta})/(I(L_{\alpha,\beta})+I(L_{\ell,\eta}))$

2. Spectral mapping: New image contrast of chemical bonding states

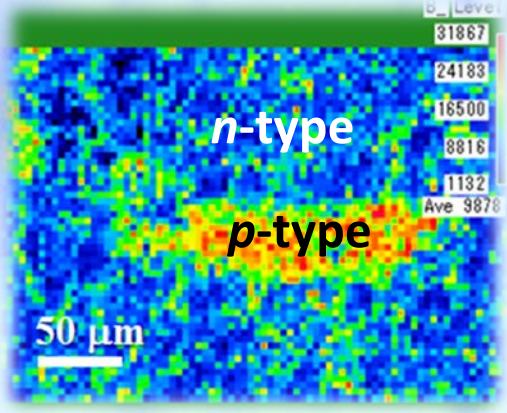

3. Improvements of SXES method
   / Detection efficiency: x5 improvement is possible for B-K emission
   / HR-SXES is under construction: 0.3 eV@~190eV
   / Energy calibration: C-K of Graphite sp^2-σ is 277.0 eV
   B-K of pure B (β-r-B) is 185.3 eV